THE INVESTIGATION OF MOLECULAR MECHANISMS IN PHOTODYNAMIC ACTION AND RADIOBIOLOGY WITH NANOSECOND FLASH PHOTOLYSIS AND PULSE RADIOLYSIS

Progress Report
for Period October 1, 1980-September 30, 1981

Leonard I. Grossweiner

Illinois Institute of Technology
Chicago, Illinois 60616

June 1981

Prepared for
THE UNITED STATES DEPARTMENT OF ENERGY
UNDER CONTRACT NO. DE-AC02-76EV02217

COO-2217-38

DISCLAIMER

Table of Contents

Abstract

Laser flash photolysis experiments have led to a new mechanism for the ultraviolet photolysis of aqueous tryptophan (Trp), indole (Ind) and certain indole derivatives. Excitation at 265 nm leads to photoionization via a pre-fluorescent state with thermal activation. The internal conversion to the fluorescent state parallels the population of a new intermediate, state X, which may be photoionized at 530 nm. State X for Trp is formed with quantum yield >0.4 at 265 nm and its lifetime is ~ 10^{-9} sec. It may be responsible for monophotonic reactions sensitized by Trp in which free hydrated electrons are not involved. The available data indicates that the formation of state X is favored by the side chain and the aqueous environment, suggesting a charge-transfer complex with the medium.

A new formula is proposed for predicting enzyme inactivation quantum yields from the composition:

$$\Phi_{in} = \Gamma_{trp} f_{trp} \eta_{trp} + \Gamma_{cys} f_{cys} \eta_{cys}$$

where Γ is the fraction of essential residues, f is the fractional light absorption, and η is the quantum yield for destruction of the residue in the enzyme. The predictions are in good agreement with measurements on six important enzymes at 254 nm and 280 nm, taking $\eta_{trp} = 0.05$ at both wavelengths (from initial photoionization yields) and $\eta_{cys} = 0.20$ at 254 nm and 0.13 at 280 nm (from cystine destruction in glutathione). The correlation indicates that direct photolysis of essential tryptophanyl and cystinyl residues are the key inactivating processes and that electron or energy transfer are not important in these enzymes.

Kinetics models have been developed and tested for important stages in the photosensitization of DNA to near-ultraviolet radiation by furocoumarin compounds currently used for PUVA therapy (psoralen plus UV-A) of psoriasis and other human skin diseases. Experiments on photobinding of psoralen (Ps) and 8-methoxypsoralen (8-MOP) to calf thymus DNA are consistent with the assumption that equilibrium dark complexing of the furocoumarin to the DNA is a precondition for the formation of covalent monoadducts and cross-links. A new analysis

based on "large target" diffusion kinetics indicates that singlet oxygen (O_2^*) generated by the unbound furocoumarin has a high probability for reaching the DNA surface. The yields of photoadducts produced by the dark-complexed component are in good agreement with published data for photobinding Ps to calf thymus DNA and photobinding 8-MOP to yeast cell DNA *in vivo*. The general development applicable to repair-competent systems predicts survival curves for *E. coli* K-12 strains exposed to black light in the presence of 8-MOP . The analysis leads to "repair-lethality" parameters indicating that DNA polymerase I is involved in the repair of furocumarin monoadducts and that 8-MOP monoadducts make a significant contribution to lethality in the wild type strain and are the dominant lethal lesions in repair-deficient strains, *uvrB* and *recA* .

Singlet oxygen generation by furocoumarins has been investigated with liposomes and human erythrocytes (rbc). Results obtained with 3-carbethoxypsoralen (3-CPs), an experimental alternate PUVA sensitizer claimed to be non-tumorigenic, show that 3-CPs interacts with liposome and rbc membranes in the dark. Negative results in control experiments with 8-MOP suggest the possibility of membrane damage with 3-CPs that should be further investigated. Related experiments on photosensitized inactivation of lysozyme have shown that 3-CPs does not generate O_2^* . However it is much more readily photolyzed than 8-MOP under anaerobic conditions leading to short-lived products that induce inactivation of the enzyme.

Studies on photosensitization of egg lecithin liposomes by methylene blue (MB) incorporated in the membrane have led to the new result that membrane lysis is a two-stage process. The first stage induced by red light irradiation leads to membrane damage initiated by O_2^* . Membrane lysis takes place in the dark, second stage under the action of mild hydrodynamic stress, such as slow gas bubbling.Similar results were obtained with MB in the external aqueous medium, suggesting that the role of hydrodynamic stress should be reexamined in prior work on photosensitization of liposomes.

Reporting of Research

Journal Articles and Books

1. The Effect of Dark Complexing on the Photosensitized Formation of 8-Methoxypsoralen Cross-links with DNA.
   L.I.Grossweiner and W.V.Sherman;
   Photochemistry and Photobiology, Vol.29, pp.697-699 (1980)
2. Multiple Pathways of Tryptophan Photoionization.
   L.I.Grossweiner, A.M.Brendzel and A.Blum;
   Chemical Physics, Vol.00, pp.000-000 (1981).
3. Dark Membrane Lysis and Photosensitization by 3-Carbethoxypsoralen.
   R.Muller-Runkel and L.I.Grossweiner;
   Photochemistry and Photobiology, Vol.33, pp.399-402 (1981).
4. Sensitivity of DNA Repair-Deficient Strains of Escherichia coli K-12 to Various Furocoumarins and Near-Ultraviolet Radiation.
   L.I.Grossweiner and K.C.Smith;
   Photochemistry and Photobiology, Vol.33, pp.317-324 (1981).
5. Kinetics of Furocoumarin Photosensitization of DNA by Near-Ultraviolet Radiation.
   L.I.Grossweiner;
   Photochemistry and Photobiology, Vol.00, pp.000-000 (1981).
6. Photodynamic Damage to Egg Lecithin Liposomes.
   R.Muller-Runkel, J.Blais and L.I.Grossweiner;
   Photochemistry and Photobiology, Vol.33, pp.683-688 (1981).
7. Photosensitization of Biomolecules In Vivo.
   L.I.Grossweiner;
   In "Oxygen and Oxyradicals in Chemistry and Biology" (Ed. M.A.J. Rodgers and E.L.Powers), Academic Press, New York, 1981, pp.000-000.
8. Primary Processes in the Photochemistry of Proteins.
   L.I.Grossweiner, A.Blum and A.M.Brendzel;
   In "Proceedings of the 8th International Congress on Photobiology", Strasbourg, July 20-25, 1980, Plenum Press, London, 1981.
9. Primary Mechanisms of Furocoumarin Photosensitization.
   L.I.Grossweiner;
   In "Proceedings of the Third International Symposium on Psoriasis", (Ed. E.M.Farber and A.J.Cox), Grune and Stratton, 1982, pp.000-000.

Meetings

1. Third International Psoriasis Symposium , Stanford University School of Medicine, July 13-17,1981.
   "Primary Photosensitization Mechanisms" (Plenary Lecture)
   L.I.Grossweiner
2. Ninth Annual Meeting, American Society for Photobiology, Williamsburg, Va., June 14-19, 1981.
   a. "Multiple Pathways of Tryptophan Photolysis" (Symposium)
      L.I.Grossweiner
   b. "Photoionization of Aqueous Tryptophan and Indole"
      A.Blum, A.M.Brendzel and L.I.Grossweiner

American Society for Photobiology (continued)

c."Mathematical Modeling of Furocoumarin Photosensitization"
L.I.Grossweiner

d."Photodynamic Sensitization of Liposomes to Hydrodynamic Stress"
J.B.Grossweiner and L.I.Grossweiner

Thesis

Ph.D. Dissertation, "Liposome Damage by Oxygen Intermediates and 3-Carbethoxypsoralen"
Renate Muller-Runkel;
Illinois Institute of Technology, May, 1981.

Research Progress

1. Primary Processes in the Photochemistry of Proteins

The effects of ultraviolet radiation on proteins offers one of the most interesting challenges in the field of photochemistry, with important implications for UV radiation damage in biological systems. The overall objective is to follow the pathways of energy deposition and chemical changes leading to permanent protein damage. Most of the emphasis has been given to enzymes, globular proteins whose catalytic activity depends on the specific sequence of amino acid residues leading to an active conformation in the appropriate ranges of temperature and pH . Proteins provide excellent systems for studying intra-molecular energy and electron transfer processes under conditions where diffusional reactions of the amino acids are inhibited. Progress has been made on two aspects of this problem during the previous year. At the experimental level, the preliminary results on laser flash photolysis of aqueous tryptophan and related indole derivatives have been extended, leading to a new mechanism of tryptophan photochemistry. In addition, a new phenomenological theory of enzyme inactivation quantum yields was developed, with predictions in close agreement to experiment for a number of important enzymes.

A. Multiple Pathways of Tryptophan Photoionization Based on Laser Flash Photolysis

The prior Progress Report (June 1980) reported the surprising observation that the photoionization of aqueous tryptophan, tyrosine, several indole derivatives, and several enzymes is enhanced many-fold when strong 530 nm radiation is superimposed on the exciting 265 nm radiation. Based on the dependence of the hydrated electron (e^-_{aq}) yields on laser intensity and temperature, it was proposed that photoionization of Trp(aq) may occur via a thermally-activated monophotonic pathway and a biphotonic pathway. Finnstrom et al. [1] reported a similar 530 nm enhancement effect for Trp(aq) and proposed that the thermally-equilibrated, first excited singlet state (S_1) is the intermediary for the biphotonic process. However, we have shown that this cannot be correct, because the e^-_{aq} yield is not

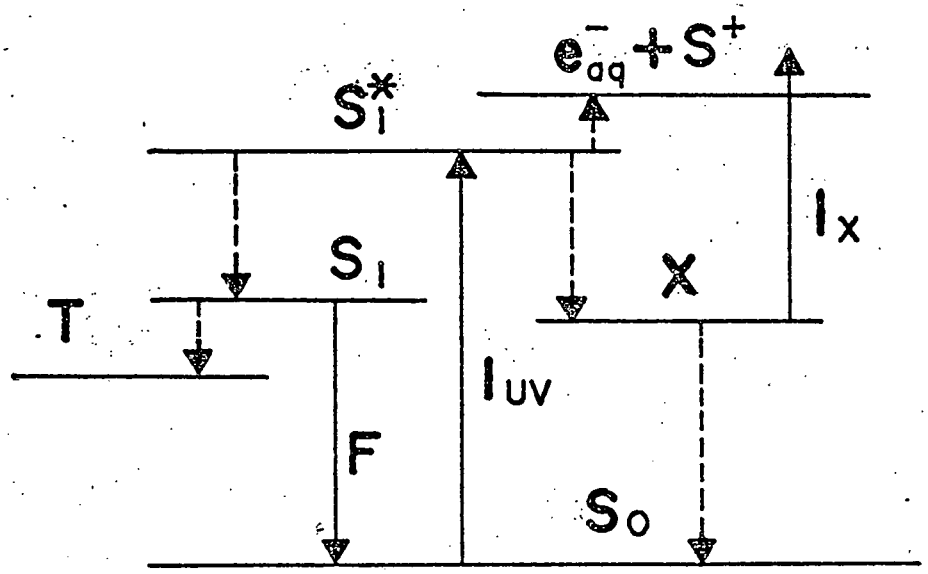

Figure 1. Scheme for photoionization of aqueous tryptophan. Monophotonic ionization excited at 265 nm (I_{uv}) takes place via pre-fluorescent state S_1^*. Biphotonic ionization at 530 nm (I_x) at 530 nm takes place via state X.

affected by the presence of high bromide ion concentrations, while the fluoresence is strongly quenched (Table 1). This data provides evidence that neither monophotonic nor biphotonic ionization of Trp(aq) takes place via S_1 or the lowest triplet state (T). These findings are consistent with other results indicating that the monophotonic ionization of Trp(aq) takes place in a pre-fluorescent state[2-4]. However, excluding S_1 and T as the biphotonic ionization intermediaries, a major question arises as to the nature of the state involved.

The kinetics model based on the above considerations is shown in Fig.1, where state X is the unknown biphotonic ionization state. The quantum yield for population of state X (Φ_x^0) can be estimated from the quasi-steady state approximation for laser flash photolysis conditions, assuming that its lifetime (τ_x) is much shorter than the laser pulse duration of 17 ns. In this case, the e^-_{aq} concentration during the laser pulse is given by:

$$C_e = E_{uv}[\Phi_e^0 + \Phi_x^0 \, Y/(1 + Y)] \qquad (1)$$

where E_{uv} is the 265 nm pulse energy, Φ_e^0 is the monophotonic ionization quantum yield, and Y is an intensity parameter for combined 265 nm and 530 nm excitation defined as: $Y \equiv \sigma_x \tau_x I_x$, where σ_x and τ_x are the optical absorption cross-section (530 nm) and lifetime of state X and I_x is the 530 nm intensity (quanta cm^{-2}). The ratio of C_e for 530 nm plus 265 nm excitation to C_e for 265 nm excitation gives the enhancement factor (K_e) as:

$$K_e = 1 - (\Phi_x^0/\Phi_e^0)[Y/(Y+1)] \qquad (2)$$

Since $(\Phi_x^0 + \Phi_e^0 + \Phi_T^0 + \Phi_F^0) = 1$, where Φ_T^0 is the intersystem crossing efficiency for Trp(aq), (estimated as 0.3 from Table 2), and Φ_F^0 is the fluorescence efficiency (0.14), Eq.(2) leads to the lower limit on Φ_x^0 and the upper limit on Φ_e^0 . The data for Trp(aq) gave $K_e = 3.7 \pm 0.5$ at 25°C (8 runs) and therefore, $\Phi_x^0 > 0.41$ and $\Phi_e^0 < 0.15$.

The high value of Φ_x^0 corresponds to the efficient population of state X even for monophotonic (low intensity) excitation. The minimum lifetime (τ_x) for detection under our laser conditions is about 0.5 ns . The structure of state X is unknown. It may correspond to the charge-transfer complex proposed by Truong [5] from luminescence and absorption measurements of tryptophan at high salt concentration.

TABLE I

Effect of Bromide Ion on Aqueous
Tryptophan and Indole Photoinization

System	F[a)]	$\Phi(e^-_{aq})$[b)]	Enhancement (K_e)
400μM Trp	1.0	1.0	3.7±0.5
400μM Trp+0.5 M Br^-	0.24	1.2	3.6±0.6
400μM Trp+3.0 M Br^-	0.11	0.9	3.6±0.6
300μM Ind	1.0	1.0	1.5±0.3
300μM Ind+1.5 M Br^-	0.27	0.9	1.4±0.3

a) Fluorescence efficiency excited at 265 nm relative to aqueous tryptophan or indole as unity.

b) 265 nm excitation, nitrogen saturation, 50 ns delay, relative to no bromide ion present.

TABLE II

Transient Product Yields From
Flash Photolysis of Aqueous Tryptophan

Transient species	265 nm*	265+530 nm*	Enhancement (K_e)
e^-_{aq} a)	4.9	17	3.4
Trp^+ b)	4.6	15	3.3
$Trp^\bullet$ c)	5.5	17	3.1
^3Trp d)	19	19	1

a) 100 ns delay, N_2-saturation; based on $\varepsilon(e^-_{aq})$ = 14400 $M^{-1}cm^{-1}$ at 630 nm [E.M. Fielden and E.J. Hart, Trans. Faraday Soc. 63, 2975 (1967)]

b) 100 ns delay, N_2O-saturation; based on $\varepsilon(Trp^+)$ = 2600 $M^{-1}cm^{-1}$ at 580 nm [L.I. Grossweiner and J.F. Baugher, J. Phys. Chem. P1, 93 (1977)]

c) 3300 ns delay, N_2O-saturation; based on $\varepsilon(Trp^\bullet)$ = 1800 $M^{-1}cm^{-1}$ at 510 nm [Ibid.]

d) 100 ns delay, N_2O-saturation; based on $\varepsilon(^3Trp)$ = 3600 $M^{-1}cm^{-1}$ for indole(aq) at 440 nm [R. Santus, private communication]

* Product yields in micromolar

Although photoionization is the dominant initial photochemical reaction of Trp(aq), important processes have been identified in which free e^-_{aq} is not involved, e.g. the photosensitized splitting of thymine dimers in DNA [6]. These reactions are promoted by molecular complexes of Trp peptides with DNA and may involve X as the Trp electron-transfer state.

The relative solvated electron yields in water-ethanol solutions are shown in Fig.2, where the values for 265 nm excitation alone have been reduced by 0.6 to account for the absorption of the green filter used in these measurements (Corning C.S. No. 7-54). The apparent enhancement factor for 100% ethanol is 1.5 . However, if photoionization at 265 nm were entirely biphotonic, then the filter would reduce the electron yield by 1/0.36 = 2.8 , compared to the measured value of 1.5/.6 = 2.5 . (The 530 nm excitation would have no effect in this case.) Therefore, the possibility of only biphotonic ionization of tryptophan in ethanol cannot be excluded. This possibility is supported by data showing negligible electron enhancement in raising the temperature from 20°C to 70°C and an approximate square dependence of the yield on laser intensity. These results indicate that the formation of state X is highly solvent dependent, with a low yield in ethanol compared to water.

The value $\Phi^0_e < 0.15$ deduced from the above analysis may be compared with published values of initial e^-_{aq} yields for Trp(aq) of 0.04 to 0.10 at 265 nm (summarized in [7]). It may be concluded that relatively little e^-_{aq} decay takes place from the time of monophotonic ionization in the pre-fluorescent state until about 10 ns. The estimated product yields in Table 2 , based on Fig.2 of the preceding Progress Report and independent values of the extinction coefficients, show that e^-_{aq} and radical cation (Trp^+) yields at 100 ns are equivalent and the same as the neutral radical (Trp•) yield at 3.3 μs. These results provide additional evidence for a relatively slow recombination of e^-_{aq} and Trp^+ as proposed in our prior work [8-10]

Similar monophotonic and biphotonic ionization pathways have been identified with aqueous indole and indole derivatives, with a trend towards higher values of K_e with increasing length of the side chain: indole(1.5), 3-methylindole(1.6), indole-3-ethanol(3.5), indole-3-acetic acid(2.8), indole-3-propionic acid(3.0), tryptamine(2.1), tryptophan(3.7). Quite high values of K_e have been obtained with

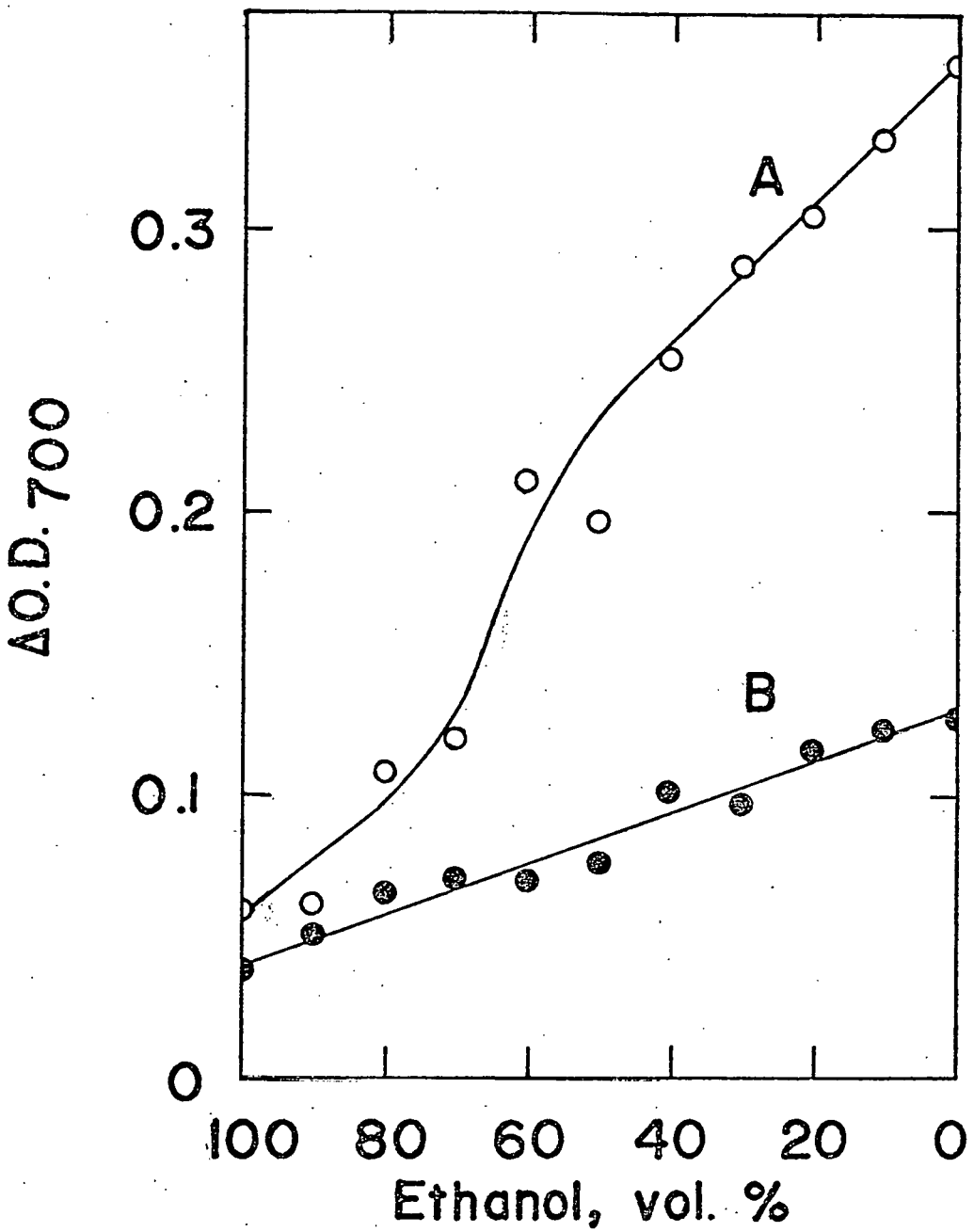

Figure 2. Solvated electron yield from 400 μM tryptophan in water-ethanol solutions.
(A) excited 265 nm + 530 nm
(b) excited 265 nm (corrected by 0.6 filter factor)

enzymes, which is the subject of current research.

B. Enzyme Inactivation Quantum Yields

Many attempts have been made to predict the quantum yields of enzyme inactivation by ultraviolet radiation based on the overall composition. The model of McLaren [11] represents one limiting case, where each absorbing residue contributes to the inactivation quantum yield (Φ_{in}) according to its extinction coefficient and the quantum yield for destruction of the corresponding amino acid in aqueous solution. A different approach is that of Dose [12], in which only the essential residues are considered and energy transfer from aromatic residues to essential cystine residues is included. Both of these models provide good predictions for a number of enzymes at 254 nm irradiation. They precede our flash photolysis studies showing that photoionization of tryptophanyl and tyrosinyl residues is the principal initial act in proteins, where the photoelectrons are stabilized as e^-_{aq} and may also be transferred to disulfide bridges within the molecule [13]. It has been found that quite good values of Φ_{in} can be predicted at 254 nm and 280 nm by assuming that direct photodisruption of essential tryptophanyl and cystinyl residues are the most important inactivating processes. The working relation is:

$$\Phi_{in} = \Gamma_{trp} f_{trp} \eta_{trp} + \Gamma_{cys} f_{cys} \eta_{cys} \qquad (3)$$

where Γ is the fraction of essential residues of the given type, f is the fractional absorption by all residues of that type in the enzyme, and η is the quantum yield for destruction of the residue in the enzyme. The results for six important enzymes are given in Table III. The value $\eta_{trp} = 0.05$ was used for all enzymes at 254 nm and 280 nm, based on flash photolysis data obtained in this laboratory (Table IV). (Measurements of permanent tryptophan destruction in proteins also lead to $\eta_{trp} \simeq 0.05 \pm 0.03$ [14].) The value of η_{cys} was taken as 0.20 at 254 nm and 0.13 at 280 nm, based on experimental quantum yields for destruction of glutathione [15]. The values of f_{trp} and f_{cys} were calculated from the corresponding amino acid extinction coefficients, and the Γ values are based on biochemical data and pulse radiolysis radical-anion probe methods, e.g. the review of

TABLE III

Calculation of Enzyme Inactivation Quantum Yields
Based on Essential Cystyl and Tryptophyl Residues

Enzyme	Γ_{trp}*	Γ_{cys}*	254 nm		280 nm	
			Φ_{in}(calc)	Φ_{in}(exptl)	Φ_{in}(calc)	Φ_{in}(exptl)
lysozyme	3/6	2/4	0.028	0.024[a]	0.023	0.023[g]
trypsin	1/4	2/6	0.015	0.020[b]	0.009	0.010[h]
papain	1/5	0/3	0.006	0.006[c]	0.006	0.003[c]
carboxypeptidase A	1/6	0/1	0.005	0.005[d]		
subtilisin Carlsberg	0/1	-	0.000	0.007[e]		
ribonuclease	-	2/4	0.029	0.030[f]	0.004	0.007[f]

* essential residues/total residues

a) D. Shugar, Biochim. Biophys. Acta 8, 302 (1952).
b) K. Dose, Photochem. Photobiol. 6, 423 (1967).
c) K. Dose and S. Risi, Ibid. 15, 43 (1972).
d) R. Piras and B.L. Vallee, Biochemistry 6, 2269 (1967).
e) A.D. McLaren and O. Hidalgo-Salvatierra, Photochem. Photobiol. 3, 349 (1964).
f) T.K. Rathinasamy and L.G. Augenstein, Biophys. J. 8, 1275 (1968).
g) L.I. Grossweiner and Y. Usui, Photochem. Photobiol. 13, 195 (1971).
h) W.A. Volkert and C.A. Ghiron, Ibid. 17, 9 (1973).

TABLE IV

Initial Product Yields from 265 nm Laser Flash Photolysis

Enzyme	$\Phi(Trp^{\bullet})^{\#}$	$\Phi(Tyr^{\bullet})^{\#}$	$\Phi(RSSR^{\bullet -})^{\#}$	$\Phi(e^-_{aq})^{\#}$	$\Sigma(\Phi_e)^{**}$
lysozyme[a]	0.031	0.000	0.007	0.019	-0.005
trypsin*	0.026	0.000	0.006	0.021	+0.001
carboxypeptidase A[b]	0.057	0.000	0.013	0.042	-0.002
subtilisin* Novo	0.054	0.018	-	0.059	-0.013
subtilisin* BPN	0.031	0.018	-	0.045	-0.004
ribonuclease[c]	-	0.016	0.000	0.016	0.000

transient product quantum yield based on absorbtion by enzyme

** electron balance

a) J.F. Baugher, L.I. Grossweiner and J.Y. Lee, Photochem. Photobiol. 25, 305 (1977).

b) W.A. Volkert and C.A. Ghiron, Ibid. 17, 9 (1973).

c) J.F. Baugher and L.I. Grossweiner, Ibid. 28, 175 (1978).

* Unreported results.

Grossweiner [14]. The good agreement in all cases except subtilisin Carlsberg, which contains no cystine and a single, non-essential tryptophan, indicates that energy and electron transfer are not important in the ultraviolet inactivation of the enzymes in Table III. However, it is not necessary that tryptophan residues are directly involved in substrate binding or the catalytic reactions. The photolysis of a tryptophanyl residue adjacent to a key residue also can induce photoinactivation. For example, Trp 199 in trypsin is adjacent to essential Ser 198, the side chain of Trp 177 in papain is in contact with His 159 of the active site, and Trp 73 in carboxpeptidase A is adjacent to Glu 72, a ligand of the essential zinc atom. In lysozyme, Trp 62, Trp 63 and Trp 108 are part of the active site crevice, and in ribonuclease A the essential Cys residues can account for photoinactivation. Table IV summarizes our available data on initial yields as obtained by laser flash photolysis. In these 6 enzymes, the yields of e^-_{aq} and the disulfide bridge electron adduct ($RSSR\cdot^-$) account for the electrons ejected from tryptophanyl and/or tyrosinyl residues at 100 ns time delay. In view of the good correlations for Φ_{in}, it does not appear that e^-_{aq} or $RSSR\cdot^-$ make a significant contribution to ultraviolet inactivation of these enzymes.

2. Primary Mechanisms in Photosensitization by Furocoumarins

The research on furocoumarin photochemistry in this laboratory is directed towards identifying the relationship of the initial reactions to the biological endpoints observed in furocoumarin photosensitization at the cellular level. New results on two aspects of the problem were obtained during the past year. An investigation of psoralen and 8-methoxypsoralen photobinding to calf thymus DNA has led to new information about the role of pre-irradiation, dark complexing on the photosensitization mechanism. The mathematical analysis based on "large target" reaction kinetics makes it possible to evaluate the possible reactions of the furocoumarin excited singlet state and the triplet state with DNA and to estimate the extent of singlet oxygen interactions. These findings are relevant to the possibility that singlet oxygen initiates mutations in microorganisms exposed to UV-A (320-400 nm) in the presence of furocoumarins, and its involvement in the tumorigenic activity of furocoumarins in laboratory animals and humans. A second study was made on membrane damage associated with furocoumarin photosensitization, emphasizing an experimental drug employed for topical photochemotherapy of psoriasis, 3-carbethoxypsoralen, which is claimed to be as effective as 8-methoxypsoralen without the risk of inducing cutaneous carcinomas. The results of this work show that singlet oxygen generation by "3-CPs" is significantly lower than "8-MOP", but there is a higher risk of membrane damage.

A. Kinetics of Furocoumarin Photosensitization In Vitro

The weak dark binding of furocoumarins to polynucleotides is a major factor in their photosensitization mechanisms. It has been assumed that the covalent furocoumarin-DNA photoaddition products are formed from the dark-complexed component, which is quite small for many furocoumarins including psoralen (Ps), 8-methoxypsoralen (8-MOP), and 3-carbethoxypsoralen (3-CPs) because of their low water solubilities. For example, the estimated fraction of DNA-complexed 8-MOP in a yeast cell suspension (5×10^7 ml^{-1}) treated with 50 μM 8-MOP is 0.3% [16]. Measurements of 8-MOP binding to calf thymus DNA were reported in the prior Progress Report (June,1980) in which the dependence of

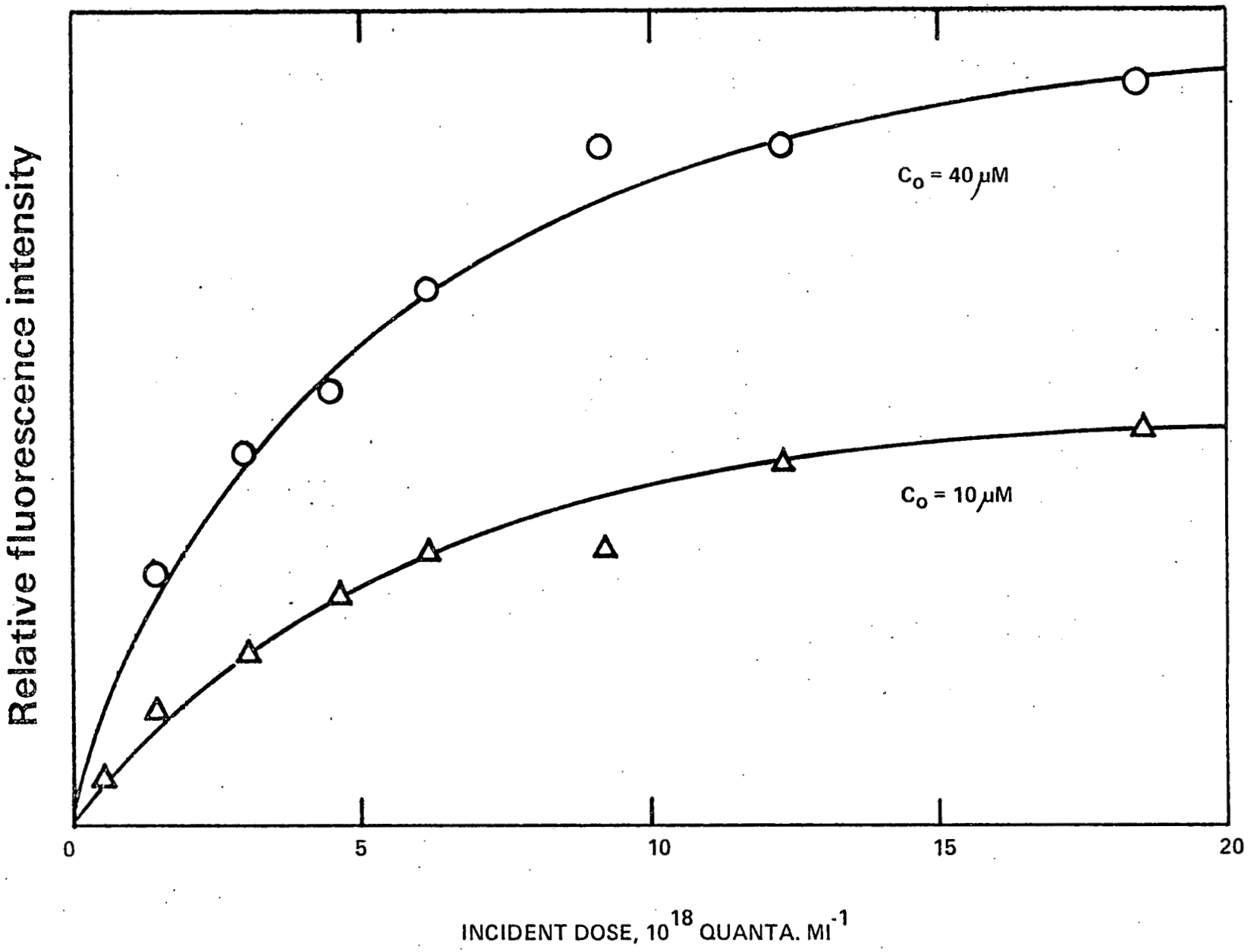

Figure 3. Formation of psoralen 4',5'-monoadducts for 1 m<u>M</u> calf thymus DNA as measured by 395 nm fluorescence after hydrolysis.

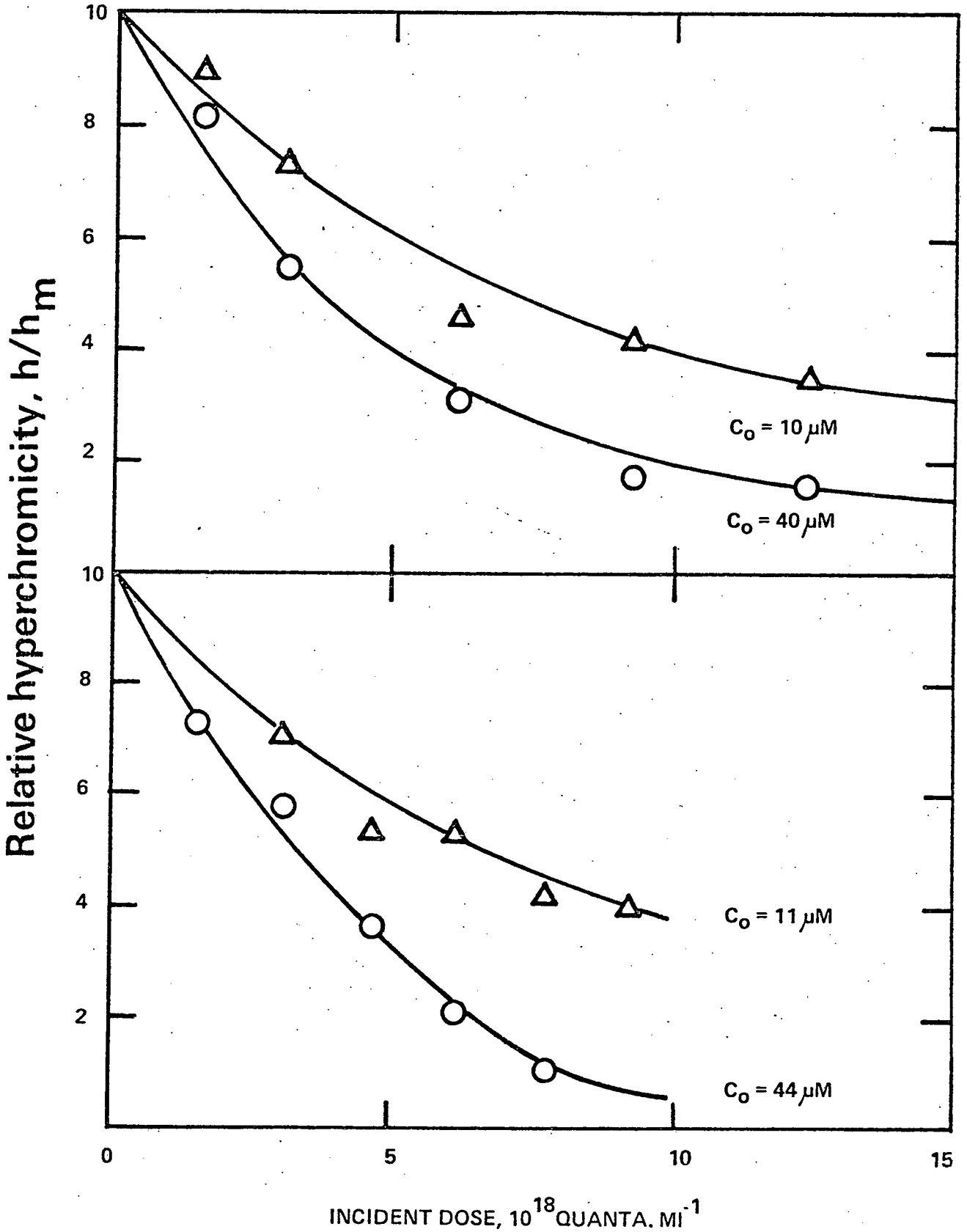

Figure 4. Formation of psoralen (upper) and 8-methoxypsoralen (lower) cross-links for 0.1 mM calf thymus DNA as assayed by hyperchromicity after thermal denaturation.

the cross-linking fluence (365 nm) on binding was measured for solutions containing 22 μM 8-MOP and differing calf thymus DNA concentrations. The results showed that the fluence required for about one cross-link per DNA molecule was constant to within ±10% for a 20-fold change in the nucleotide concentration and about 30% higher in air compared to argon saturation. The weak concentration dependence is consistent with the assumption that dark complexing is a pre-condition for photobinding, because the dose required for cross-linking should depend on $1/r^{\frac{1}{2}}$ where r is the fraction of DNA binding sites occupied by 8-MOP in the dark. However, this quantity is quite insensitive to the ratio of total 8-MOP to total nucleotides, apparently explaining the experimental result.

These studies were continued during the past year, where the formation of 8-MOP cross-links and PS monoadducts and cross-links on 365 nm fluence were measured for different initial furocoumarin and nucleotide concentrations. Typical data for the growth of Ps 4',5'-monoadducts are shown in Fig.3, based on a fluorescence assay technique [17]. The growth of PS and 8-MOP cross-links was assayed with the thermal denaturation method [18], in which the number of cross-links per DNA molecule is related to hyperchromicity changes when the DNA is heated to 85°C and cooled; typical data are shown in Fig.4 . The summary of the 8-MOP cross-linking data in Table V confirms that the fluence required for 50% renaturation and denaturation (D_{50}) is independent of $r^{-\frac{1}{2}}$ to within ±15% standard deviation (SD) for a 20-fold change in the nucleotides concentration and a 4-fold change in the total 8-MOP concentration. Similar results were found for Ps cross-links; Table VI, Col.(7). Similar considerations indicate that the Ps monoadduct yield should depend on the initial amount of complexed Ps (C_b), which was valid to ±30% SD; Table VI, Col(5).

However, considerations of the kinetics shows that the implications of the data for the photobinding model may be ambiguous. If dark complexing is a pre-condition for photobinding, then the dependence of the fluorescence efficiency (after hydrolysis of the DNA) of the monoadducts (I_{fl}) on fluence (D) should follow:

$$I_{fl} \sim C_b D \qquad (4)$$

as found in Table VI, Col.(7). However, if monoadduct formation

Table V. Photobinding of 8-methoxypsoralen to calf thymus DNA.

(1)	(2)	(3)	(4)	(5)
C_N*	C_o#	D_{50}+	$D_{50}/r^{-\frac{1}{2}}$	$D_{50}/C_o^{-\frac{1}{2}}$
2200	11	11.0	0.60	0.037
2200	22	5.8	0.44	0.027
2200	44	5.0	0.53	0.033
220	22	4.0	0.43	0.019
110	11	6.2	0.50	0.021
110	22	3.9	0.43	0.018
110	44	3.0	0.43	0.020
			0.48±0.007	0.025±0.007

* concentration of nucleotides (μM)

\# concentration of 8-methoxypsoralen (μM)

\+ 365 nm fluence for $h/h_m = 0.5$ (units of 10^{-18} x photons cm^{-3})

Table VI. Photobinding of psoralen to calf thymus DNA.

(1)	(2)	(3)	(4)	(5)	(6)	(7)	(8)
C_N *	C_o #	R_{fl} †	D_{50} **	$10^{-6}R_{fl}/C_b$	$10^{-8}R_{fl}/C_oC_N$	$D_{50}/r^{-\frac{1}{2}}$	$D_{50}/C_o^{-\frac{1}{2}}$
2000	20	21	4.4	2.5	5.3	0.29	2.0
1000	10	7.8	6.8	2.9	7.8	0.36	2.2
1000	40	16	3.1	1.6	4.0	0.31	2.0
100	10	1.0	6.5	2.8	10.0	0.39	2.1
100	20	0.93	4.8	1.4	4.7	0.39	2.2
100	40	1.6	3.7	1.4	4.0	0.40	2.3
				2.1±0.7	6.0±2.4	0.36±0.05	2.1±0.2

* concentration of nucleotides (μM)

\# concentration of psoralen (μM

† initial build-up of monoadduct fluorescence (arb)

** 365 nm fluence for $h/h_m = 0.5$ (units of 10^{-18} x photons cm^{-3})

involves the homogenous reactions of excited furocoumarin molecules with DNA, then the relationship is:

$$I_{fl} \sim C_o C_N D \tag{5}$$

where C_o is the total furocoumarin concentration and C_N is the total nucleotides concentration. The data are in equally good agreement with this relationship; Table VI, Col.(6). Similarly, the pre-dark complexing model for cross-link formation leads to:

$$n_c \sim rD^2 \tag{6}$$

where n_c is the number of cross-links per DNA molecule, and the homogeneous model gives:

$$n_c \sim C_o D^2 \tag{7}$$

In Table V it is seen that Eq.(6) and Eq.(7) are in equally good agreement with experiment; Col.(7) and Col.(8), respectively. The ambiguity lies in the multiple binding formula used to estimate the dark-complexed components [19] , which can be expressed as:

$$C_b/C_o C_N = nK_b(1-f_b)/[1+(C_o K_b(1-f_b)] \tag{8}$$

where n is the number of equivalent binding sites per nucleotide, K_b is the intrinsic binding constant, and f_b is the complexed fraction of furocoumarin. The right side of this expression does not depend at all on C_N and changes very slowly with C_o for weak binding, leading to good correlations for either model.

In view of the failure of conventional kinetics to resolve the key issue as to the role of free and complex furocoumarin in photobinding, a new theory has been developed based on "large target" diffusion kinetics. This approach was previously employed in connection with the attack of short-lived species generated by ionizing radiation or photochemical radiations in the medium external to large targets [20,21]. The present application allows for direct reactions of the dark-complexed species with the DNA target plus diffusive reactions induced by the intermediates generated by the free furocoumarin in the external medium. The number of interactions with the DNA surface by externally generated species can be expressed as:

$$n^* = \Phi^* \eta^* v^* D_{abs} \qquad (9)$$

where n* is the number of surface encounters after absorbed fluence D*, Φ^* is the quantum efficiency for generating the reactive intermediate, η^* is the probability that an encounter leads to the observed event, and v* is the "reaction volume", which can be pictured as the volume of medium surrounding the DNA in which a generated species has 0.5 chance of reaching the DNA surface during its lifetime. For double-stranded DNA v* can be approximated by:

$$v^* \simeq 2\pi RL\rho[1 + \rho/2R] \qquad (10)$$

where R is the DNA radius (1×10^{-7} cm), L is the extended DNA length [$L \simeq 3.4 \times 10^{-8}(MW)_{DNA}/700$] , and ρ (cm) is the mean diffusion range of the reactive intermediate [22]. The number of monoadducts from the complexed furocoumarin for the same dose can be expressed as:

$$n_m = \Phi_m n_b D_{abs}/6.023 \times 10^{20} C_o \qquad (11)$$

where Φ_m is the quantum yield for monoadduct formation based on light absorption by the complexed furocoumarin, n_b is the original number of dark-complexed furocoumarin molecules per DNA molecule and n_m is the number of monoadducts per DNA molecule. Substituting Eq.(10) in Eq.(9) , with $n_b = (C_b/C_N[(MW)_{DNA}/350])$, gives the ratio of n* to n_m:

$$n^*/n_m = 6.4 \times 10^{13}(\Phi^*\eta^*/\Phi_m)(C_o C_N/C_b)R\rho[1+\rho/2R] \qquad (12)$$

Equation (12) shows that the ratio of external hits to monoadducts is independent of the DNA molecular weight and changes with the relative furocoumarin and DNA concentrations through a ratio that is almost constant [see Eq.(8)] and readily calculated.

The value of ρ can be taken as $(D^*\tau^*)^{\frac{1}{2}}$ where D* is the diffusion constant of the reactive intermediate and τ^* is its decay or scavenging lifetime. For the reaction of 8-MOP with calf thymus DNA, $\Phi_m = 0.007$ and $(C_o C_N/C_b) \simeq 500$ [16]. We are now in a position to evaluate Eq.(12) for the intermediates of interest:

(a) 8-MOP excited singlet state:
Taking $D^* = 5 \times 10^{-6}$ $cm^2 s^{-1}$ (from Stoke's law) and $\tau^* = 2$ ns [23] gives $\rho \simeq 1 \times 10^{-7}$cm and negligible values of n^*/n_m .

(b) 8-MOP triplet state:
For air-saturation, $\rho \simeq 4 \times 10^{-6}$ cm based on $k(T+O_2) = 1 \times 10^9$ $M^{-1}s^{-1}$ [23]. The intersystem crossing yield gives $\Phi^* = 0.14$ [24] and $n^*/n_m < 40$, which is the upper limit for $\eta^* = 1$ and a 10 µg ml^{-1} 8-MOP solution.

(c) Singlet oxygen:
For $\tau^* = 2 \times 10^{-6}$ s and $D^* = 3 \times 10^{-5}$ $cm^2 s^{-1}$, $\rho \simeq 8 \times 10^{-6}$cm and $n^*/n_m < 80$ for $\eta^* = 1$ and $\Phi^* < 0.14$.

The above results show that singlet oxygen and 8-MOP triplet states generated in the external medium by free 8-MOP can make a significant contribution to DNA damage. The latter can be ruled out for 8-MOP triplet states (but not for Ps triplet states) because of the low reactivity measured with laser flash photolysis [25]. The DNA damage induced by singlet oxygen in furocoumarin photosensitization may be of considerable biological importance and will be investigated in further work.

B. Singlet Oxygen Generation by 8-Methoxypsoralen and 3-Carbethoxypsoralen

The generation of singlet oxygen (O_2^*) was demonstrated in this laboratory for 8-MOP [23], and subsequently confirmed and extended to other furocoumarins [26,27] including Ps, 5-methoxypsoralen (bergapten, 5-MOP) and angelicin. Since O_2^* has been shown to be mutagenic in yeast cells [28], there has been speculation that O_2^* may be involved in the tumorigenic action of PUVA therapy (psoralen plus UV-A) of psoriasis with 8-MOP [29]. (The mutagenic action of 8-MOP may also be induced by error-prone repair of the 8-MOP/DNA cross-links, but the known reactivity of O_2^* with DNA, membranes and proteins provides an alternative mechanism.) In 1978, successful topical phototherapy of psoriasis was reported for 3-CPs, a derivative that does not form DNA

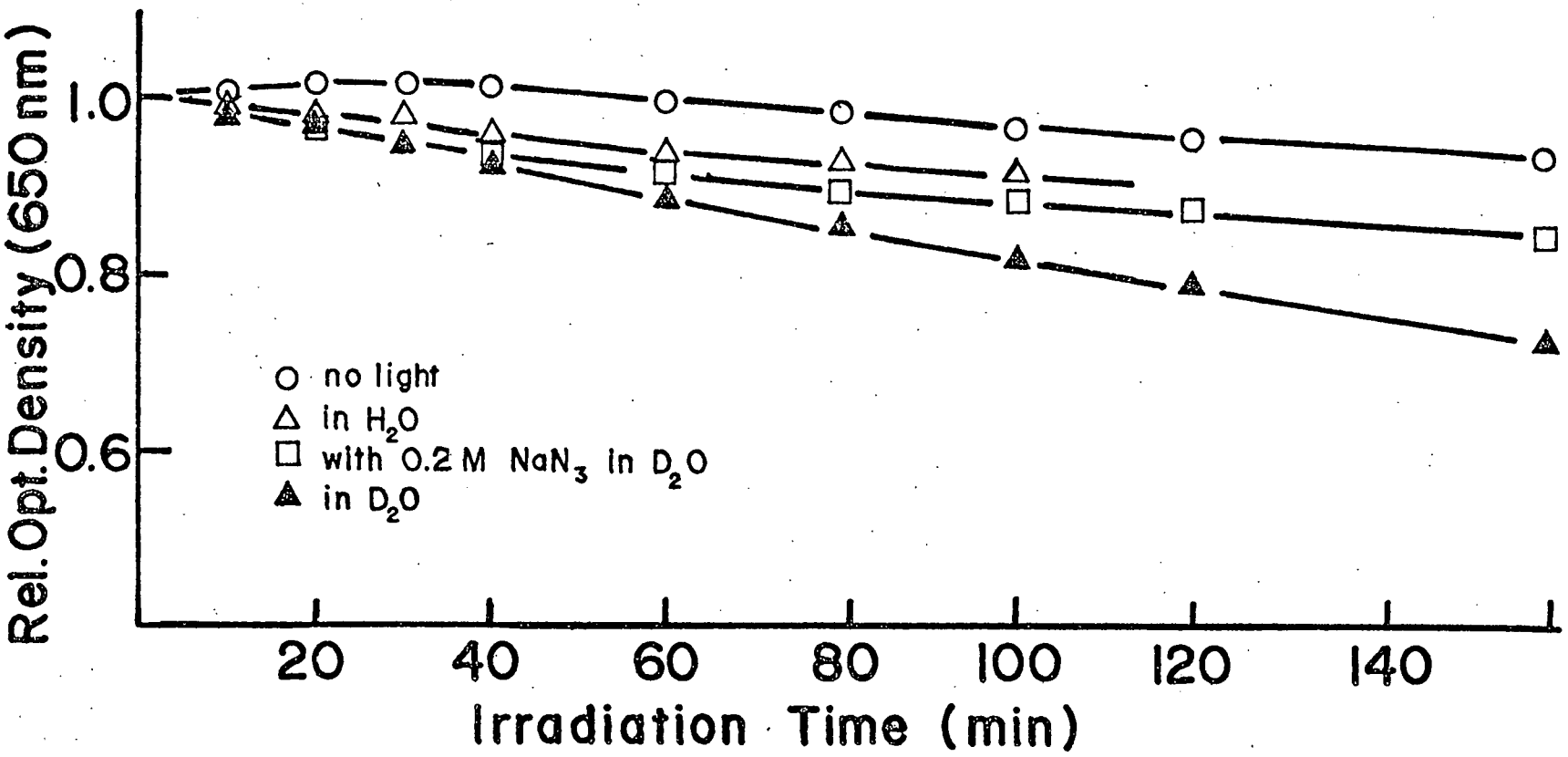

Figure 5. Photosensitized liposome damage by 160 μM 8-methoxypsoralen; oxygen-saturated, (310-390 nm).

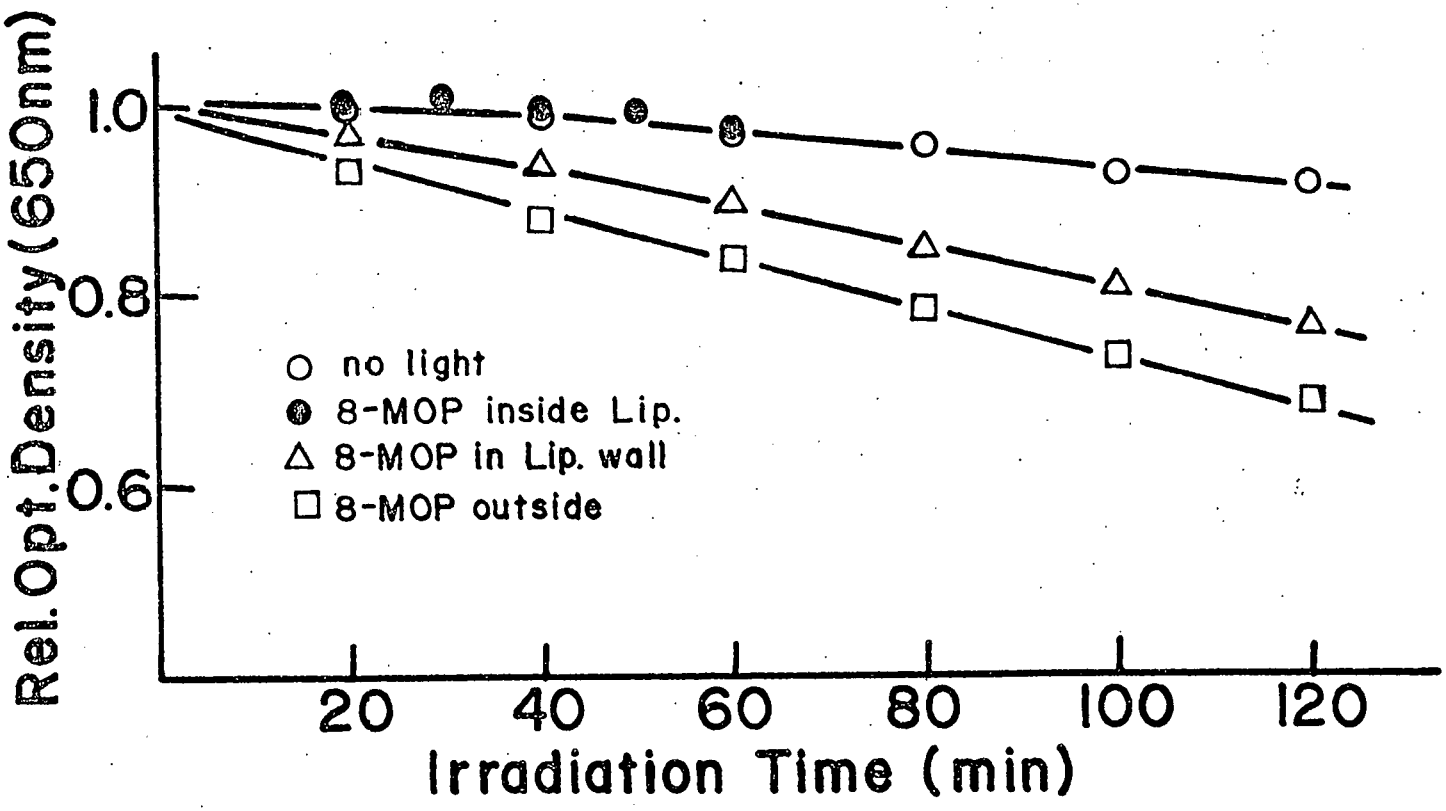

Figure 6. Photosensitization of liposomes by 8-methoxypsoralen in different liposomes phases; oxygen-saturated, (310-390 nm).

cross-links in yeast at 365 nm [30]. It is claimed that 3-CPs is not tumorigenic in mice [30], in contrast to the well-known tumorigenic activity of 8-MOP plus UV-A in laboratory animals, e.g., Ley et al. [31]. In view of the clinical importance of 8-MOP and 3-CPS as PUVA sensitizers, we undertook a study on aspects of their photosensitization mechanisms.

Based on our prior work utilizing egg lecithin liposomes as probes for O_2^* (Progress Report, June 1980), measurements were made of liposome lysis induced by the exposure to UV-A in the presence of 8-MOP and 3-CPs. Typical results in Fig.5 for 160 μM 8-MOP irradiated with a 200-W h.p. Hg arc through a Corning C.S.No.7-39 filter (310-390 nm) show the protection by azide ion and enhanced lysis in D_2O characteristic of O_2^* participation. The relatively slow lysis rate compared to methylene blue sensitization (Progess Report, June 1980) is characteristic of the low O_2^* yield from 8-MOP [26]. The results in Fig.6 show that lysis is more efficient for 8-MOP in the external medium than for the same concentration entrapped within the liposome or incorporated in the liposome membrane. The equivalent experiments with 3-CPs were unsuccessful because of the dark interactions of 3-CPs with the lipid membrane. As reported in the prior Progress Report, it was found that 3-CPs exerts a detergent action on egg lecithin liposomes leading to dark lysis under mild bubbling in the dark. The inhibition of the dark lysis in the presence of 9:1 water-ethanol was explained by stabilization of the 3-CPs in the aqueous phase.

The question of O_2^* generation by 3-CPs was investigated using the inactivation of hen lysozyme as an alternative probe [23]. The results in Fig.7 show that the inactivation rate is much faster under argon saturation (curve B) than with oxygen saturation (curve C) . In contrast, for 8-MOP photosensitization, the inactivation rate in argon and D_2O (curve D) is slower than for O_2 saturation (curve E) as expected for O_2^* involvement. However, for 3-CPs the dependence of the inactivation rate (T_{37}) on lysozyme is characteristic of the kinetics where the inactivating agent is generated in the external medium , Fig.8 [14]. It is most likely

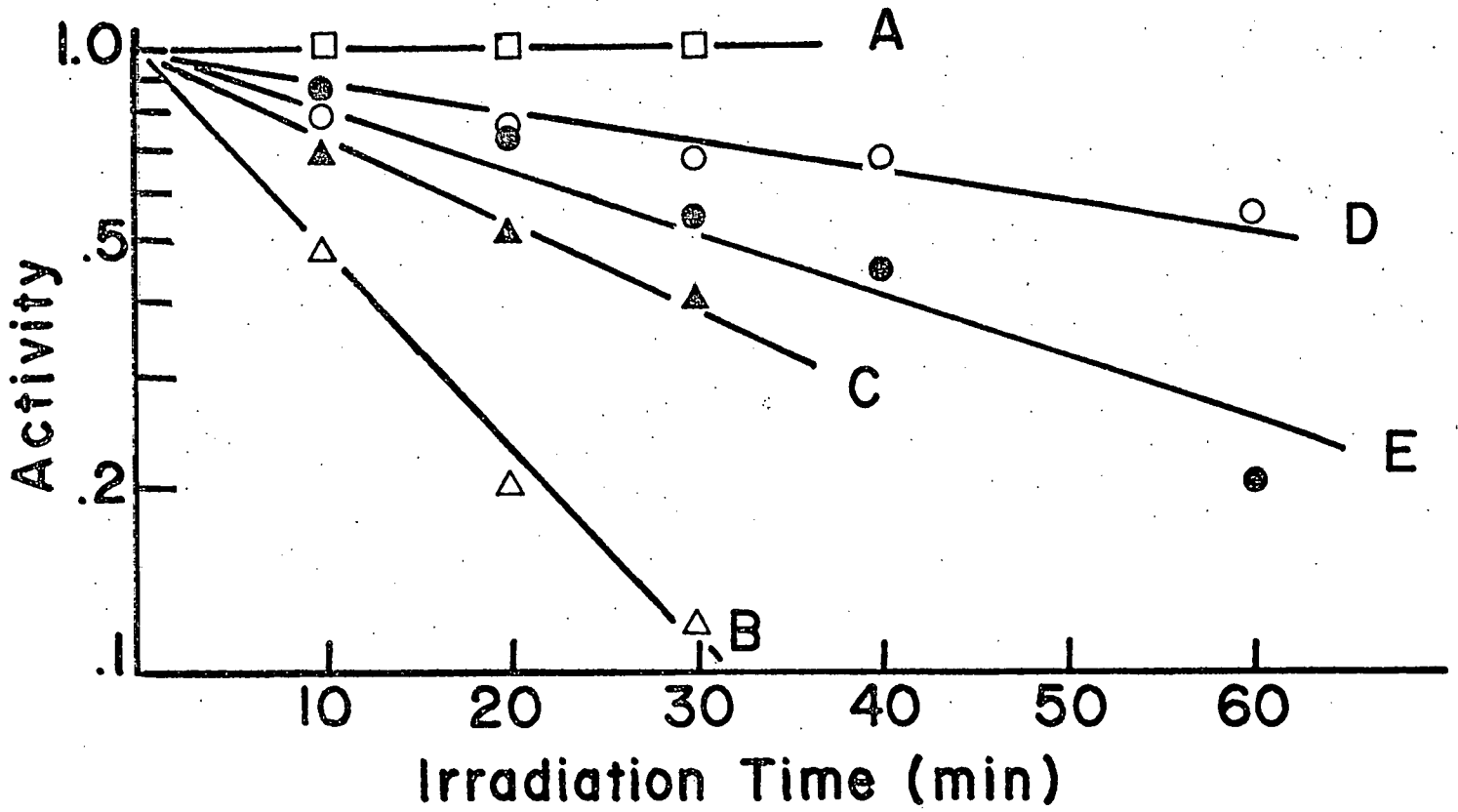

Figure 7. Photosensitization of the inactivation of hen lysozyme. A. dark, O_2-bubbled with 40 μM 3-CPs; B. irradiated, argon-bubbled with 40 μM 3-CPs; C. irradiated, O_2-bubbled with 40 μM 3-CPs; D. irradiated, argon-bubbled with 37 μM 8-MOP; E. irradiated, O_2-bubbled with 37 μM 8-MOP.

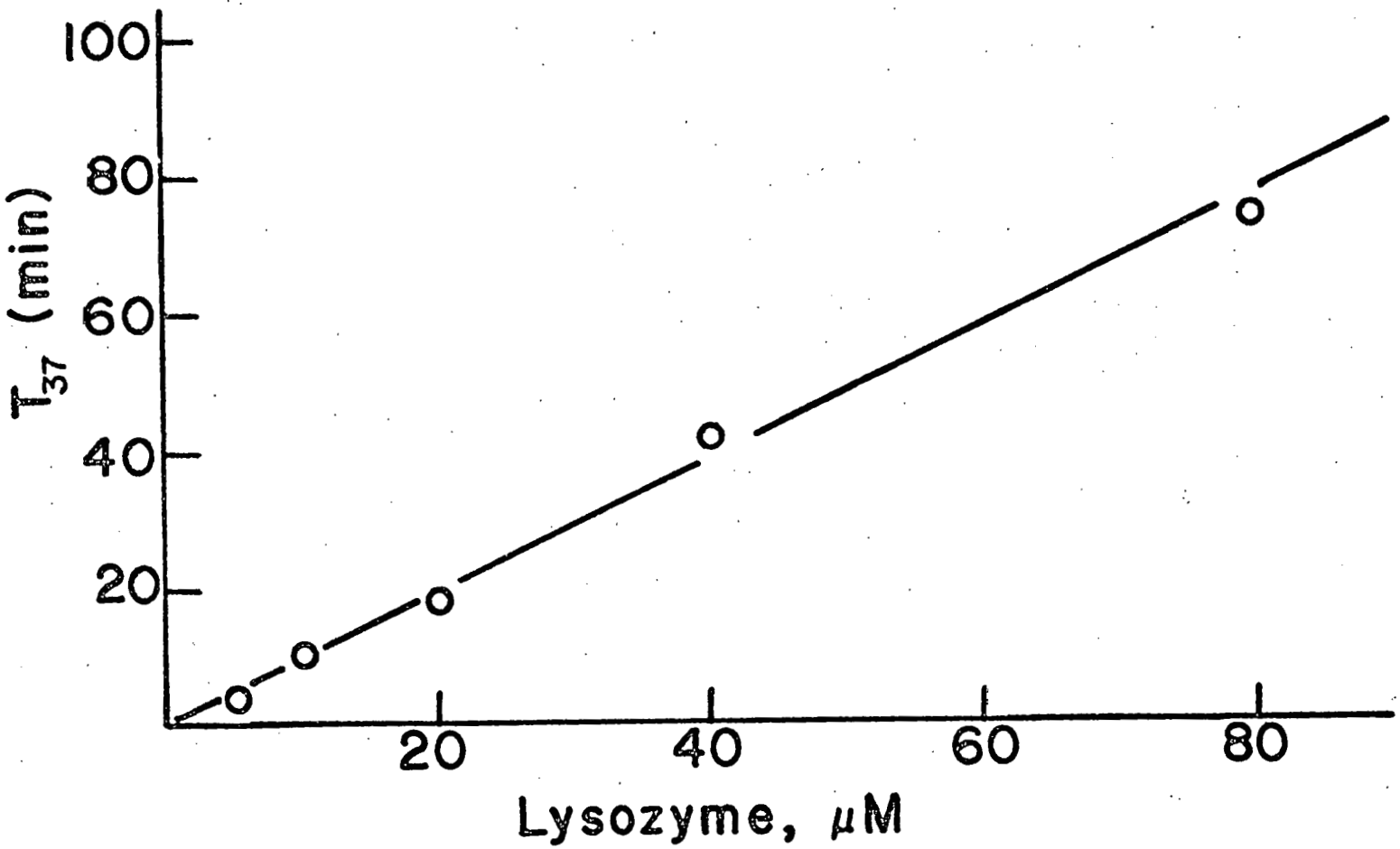

Figure 8. Dependence of lysozyme inactivation rate (T_{37}) on enzyme concentration for inactivation by 40 μM 3-CPs; argon-bubbled, (310-390) nm.

that reactive free radicals are the major inactivating agent for 3-CPs, consistent with the rapid photolytic decomposition of 3-CPs when exposed to 365 nm radiation[32,33]. In any case, the production of O_2^* by 3-CPs must be much smaller than for 8-MOP in order to account for the protective effect of oxygen.

The dark lysis of liposomes by 3-CPs has important implications for the clinical use of this drug. The results in Fig.9 show that the dark lysis rate with argon bubbling increases with increasing 3-CPs concentration, with an apparent threshold between 22 μM and 45 μM . The liposome experiments were extended to whole human erythrocytes (rbc) in order to explore the effects with biological membranes. Two different interactions of 3-CPs with rbc were observed, each of significantly higher magnitude than with 8-MOP. A short exposure of rbc to 3-CPs in the dark induced rapid lysis, as determined by the release of hemoglobin,Fig.10. (The experimental details are summarized in [33] and the doctoral dissertation of R.Muller-Runkel, IIT, May 1981.) However, the normal lysis after long-time incubation in the dark was inhibited by 3-CPs, Fig.11. This inhibition was the same when the rbc were in the presence of 3-CPs for the full incubation period and when they were exposed to 3-CPs for 2 hrs followed by washing. Since rbc lysis is of the "colloid osmotic" type [34], the two stages may involve first the detergent effect on the lipid, paralleling the liposomes, followed by a protein interaction leading to decreased fluidity. In any case, there is little doubt that 3-CPs enters the rbc membrane and induces alterations not present in the case of 8-MOP to a significant extent.

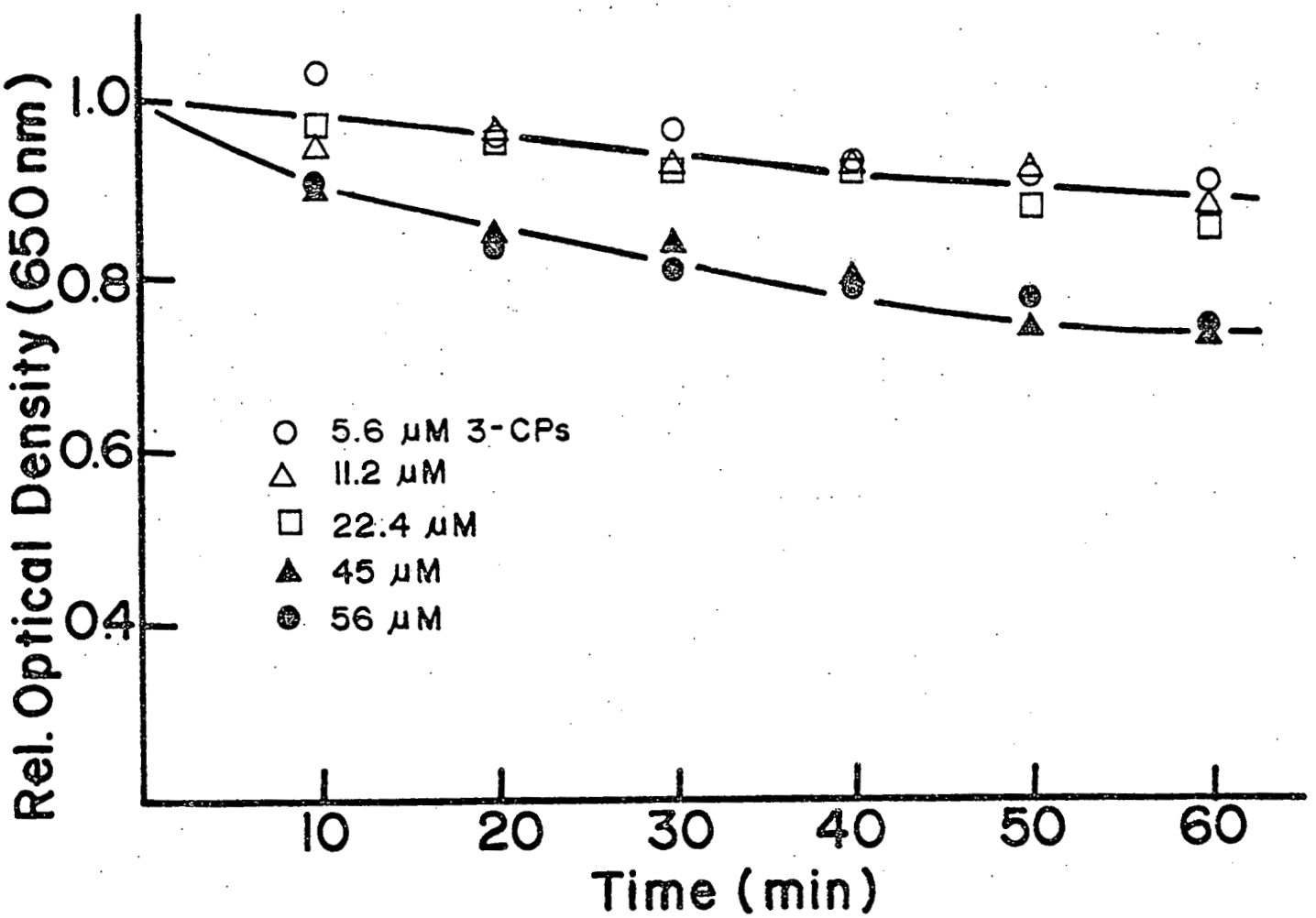

Figure 9. Lysis of liposomes in the dark by 3-CPs; argon-bubbled.

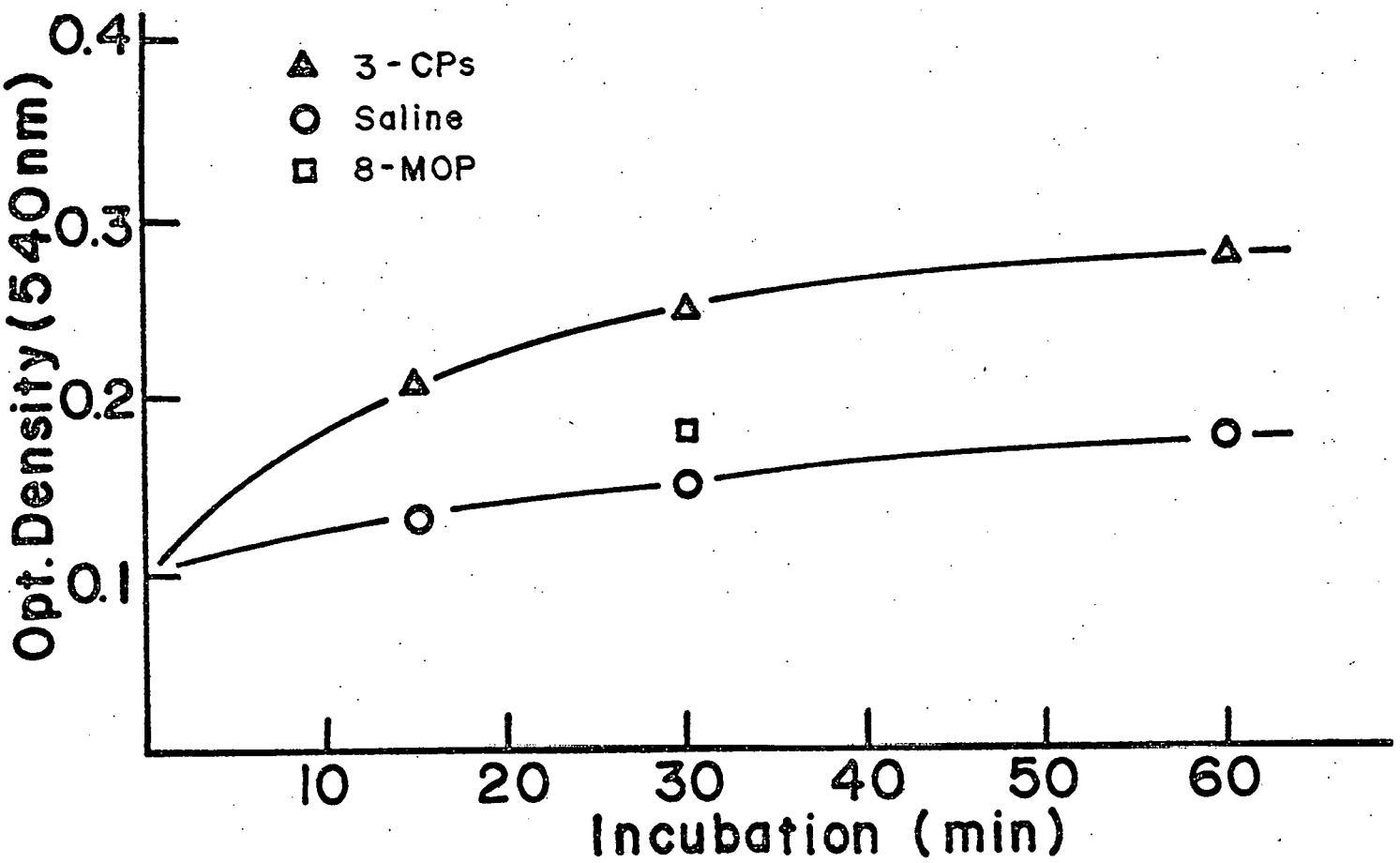

Figure 10. Dark release of hemoglobin from erythrocytes induced by 245 μM 3-CPs in saline-phosphate buffer/ethanol 1:10 (vol/vol) at 37°C and 200 μM 8-MOP (control).

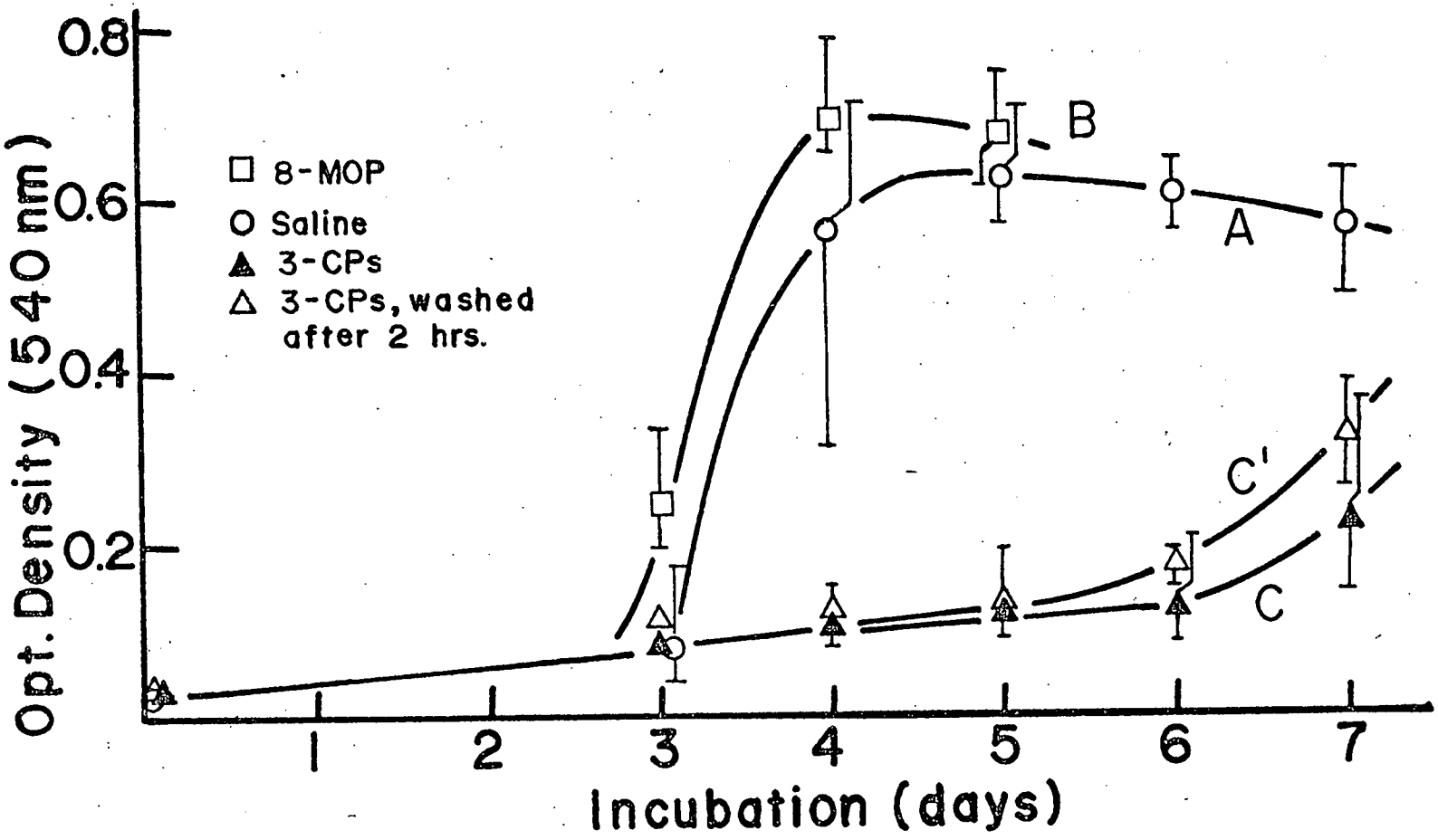

Figure 11. Effect of 3-CPs (250 μM) on stability of erythrocytes towards incubation in saline at 37°C.

C. Kinetics of Furocoumarin Photosensitization of DNA in Vivo

A new mathematical model for furocoumarin photosensitization of DNA was described in the prior Progress Report, applicable to light sources of arbitrary spectral intensity distribution and to systems of differing repair competence. This model has been refined and applied to several photosensitization systems with encouraging results. The key assumptions of the analysis are:

(a) Photobinding involves only the dark-complexed furocumarin molecules, the efficiency of which can be estimated from in vitro measurements of dark complexing constants and photobinding quantum efficiencies.

(b) The 3,4- and 4',5'-monoadducts formed from cross-linking furocoumarins, such as Ps and 8-MOP, have a certain probability for conversion to cross-links depending the binding sites, the specific furocoumarin and DNA structures, and the incident spectrum.

(c) The photoadduct yields for a given biological system prior to repair do not depend on the repair genotype of the specific strain.

The mathematical analysis follows the prior Progress Report except that differential rate equations are solved for two types of 3,4-monoadducts: those that can be converted to cross-links and those that cannot be converted to cross-links because of the binding sites, and similarly for the 4',5'-monoadducts. The complete solution for the numbers of species per DNA molecule (n_j) after scaled incident dose D' are:

$$n_f/n_f^o = e^{-D'} \tag{13a}$$

$$n_a/n_f^o = [\delta g_a/(g_a A-1)][e^{-D'} - e^{-g_a AD'}] \tag{13b}$$

$$n_a'/n_f^o = \delta(1-g_a)[1 - e^{-D'}] \tag{13c}$$

$$n_b/n_f^o = [(1-\delta)g_b/(g_b B-1)][e^{-D'} - e^{-g_b BD'}] \tag{13d}$$

$$n_b'/n_f^o = (1-\delta)(1-g_b)[1 - e^{-D'}] \tag{13e}$$

$$n_c/n_f^o = \delta g_a + (1-\delta)g_b - [\delta g_a/(g_a A-1)][g_a Ae^{-D'} - e^{-g_a AD'}] - [(1-\delta)g_b/(g_b B-1)][g_b Be^{-D'} - e^{-g_b BD'}] \tag{13f}$$

where the subscripts refer to complexed furocoumarin (f), 4',5'-monoadducts convertible and not convertible to cross-links (a,a'), similarly for 3,4-monoadducts (b,b'), and cross-links (c). The other parameters are the initial fraction of 4',5'-monoadducts (δ), the convertible monoadduct fractions (g_a,g_b), two terms relating to to the rate of cross-link formation relative to monoadduct formation (A,B) , and the scaled dose: $D' \equiv \sigma_f \Phi_m \Phi D$, where σ_f is the furocoumarin absorption cross-section (or mean cross-section for broad band excitation), Φ_m is the quantum efficiency for monoadduct formation from the complexed furocoumarin, and D is the incident fluence (see Progess Report June 1980 and ref.[16] for details.)

A preliminary test of the analysis was made for published data[35] on Ps photoadduct formation with calf thymus DNA for 365 nm radiation, using key parameters reported by the authors: $D/t = 2.9 \times 10^{16}$ photons/cm-s , $\varepsilon(Ps) = 960\ M^{-1}cm^{-1}$, $\varepsilon(4',5') = 2010\ M^{-1}cm^{-1}$, and $f_b = 0.31$ (dark-complexed Ps). The points in Fig.12 show the formation of monoadducts and cross-links and the lines were calculated from Eqs.(13) based on qualitative fitting parameters determined by the authors. The present quantitative fit indicates that the initial fraction of 4',5'-monoadducts was 0.39, that 54% of the 4',5'-monoadducts were convertible to cross-links (the 3,4-monoadducts do not absorb at 365 nm), and that the quantum yields for monoadduct formation and cross-link formation were 0.019 and 0.45, respectively. The high efficiency for converting 4',5'-monoadducts is an important conclusion of this analysis.

A more stringent test was made for photoadduct formation in DNA extracted from Saccharomyces cerevisiae (5×10^7 cells/ml) after exposure to 18.9 kJ/m^2 fluence at 365 nm in the presence of 50 μM 8-MOP [32]. The data showed that 0.0023 μg of 8-MOP were photobound to 1 μg of extracted DNA. Taking 5×10^{-14} g of DNA per cell (from the authors) and published binding constants for 8-MOP and calf thymus DNA [36] leads to $f_b = 0.0033$ and the photobinding quantum yield $\Phi_m = 0.008$. In comparison, in vitro binding of 8-MOP to calf thymus DNA, corrected for the dark complexed fractions, gave $\Phi_m = 0.007$ at 365 nm [37], in excellent agreement. These results provide strong support for the assumption that only the dark-complexed 8-MOP is photobound to DNA in vivo.

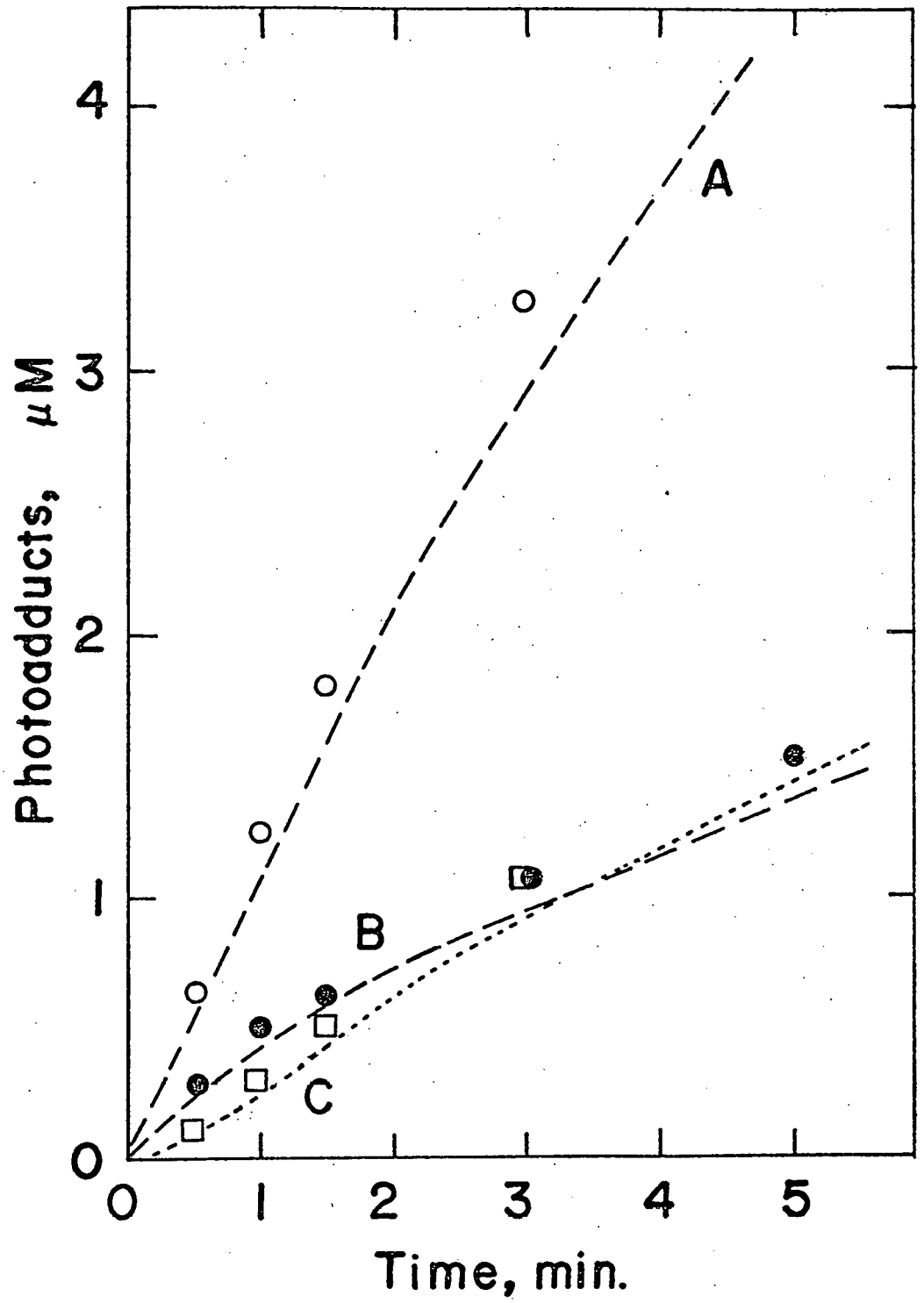

Figure 12. Fit of kinetics model to published data [35] for photobinding 54 μM psoralen to 3 mM calf thymus DNA at 365 nm; A. 3,4-monoadducts; B. 4',5'-monoadducts; C. cross-links.

Another test was made for *in vivo* photosensitization where strains of *E. coli* K-12 were exposed to fluorescent BL (black light) lamps in the presence of 10 μg/ml 8-MOP [38]. The theoretical survival curve assuming that all four types of monoadducts have equal lethality and that each non-repaired lesion contributes independently to lethality is of the form:

$$S = \exp\{-f_m n_f^0 D' [1 + \tfrac{1}{2}(f_c/f_m)A'D']\} \qquad (14)$$

where n_f^0 is the initial number of dark-complexed 8-MOP molecules per DNA molecule (calculated as 2×10^5), f_m and f_c are the probabilities that monoadducts and cross-links, respectively, are not repaired and induce lethality, and D' (defined above) was calculated taking $\Phi_m = 0.007$ and $\sigma_f = 5.7 \times 10^{-18}$ cm^2 was calculated by numerical integration of the 8-MOP absorption over the lamp spectrum (see prior Progress Report and [40]). It was assumed that $A' \equiv \delta g_a^2 A$ and n_f^0 were the same for all strains and the survival data were fitted to Eq.(14) with A' = 1.2 and the values of f_m and f_c in Table VII. (The actual fit is shown in Fig.1 of ref.[16]). The results show that monoadducts are *inherently* much less lethal than cross-links in all four strains. However, the contribution of monoadducts to lethality is significant in the wild type and *polA* strains and they are the dominant lethal lesions in the more sensitive *uvrB* and *recA* strains. The higher monoadduct lethality in the *polA* strain compared to *wild type* was attributed to the involvement of DNA polymerase I in the repair of furocoumarin monoadducts [38], which is reflected also in the high *polA* sensitivity of *E. coli* K-12 to black light plus monoadduct forming furocoumarins such as angelicin and 3-CPs [38]. The generally high monoadduct contribution to lethality is a new result of relevance to PUVA therapy with 3-CPs and in the interpretation of comparative data on lethality and mutations induced by 8-MOP, and angelicin or 3-CPs.

Table VII

Application of kinetics model to published data [38] for the photoinactivation of E. coli K-12 by black light in the presence of 46 μM 8-methoxypsoralen.

Strain	D_{37} #	f_m *	f_c **	L_m/L ##
wild type	1.30	0.00035	0.06	0.47
polA	0.85	0.0007	0.06	0.78
uvrB	0.20	0.004	0.06	0.88
recA	0.15	0.005	1.0	0.88

Inactivating fluence kJ/m^2

* Monoadduct lethality parameter

** Cross-link lethality parameter

Monoadduct fraction of lethal lesions

3. Photosensitized Lysis of Liposomes-Hydrodynamic Effects

In typical studies on photosensitization of liposomal damage, the liposomes are exposed to visible radiation in the presence of the sensitizer, which may be incorporated in the liposome membrane or dissolved in the aqueous medium. Results have been reported for various types of sensitizers including natural and synthetic pigments, e.g. the review of Grossweiner [39]. The physical state of the liposomes during photodynamic treatment has varied with the particular investigation including still suspensions [40], stirring [41] and slow bubbling with oxygen [42,43]. Recent work in this laboratory has shown that hydrodynamic effects play a major role in photosensitized liposome damage, to the extent that this factor must be considered as a controlled variable of prime importance to the photolysis mechanism. All experiments reported here were made with egg lecithin liposomes incorporating methylene blue in the membrane. The liposomes were prepared by adding methylene blue hydrochloride (MB) to a chloroform solution of the lipid (Sigma Chemical L-α-phosphatidylcholine), evaporating to dryness under nitrogen, adding 2 ml of pH 7.0 phosphate buffer, swelling 2 hours at 10°C, and washing at least six times by centrifuging at 15,000G and resuspending in the buffer. The amount of MB incorporated in the liposome membrane was estimated from the difference between the original amount and the MB in the supernatants. The irradiations were carried out in thermostated Pyrex cuvettes exposed to a 200-W Hg-Xe arc through a Corning C.S.No. 2-63 filter (λ>600 nm) and a water filter to remove infrared. The incident fluence was 117 mW/cm^2. Liposome lysis was measured by the turbiditry changes at 720 nm.

The lysis rate under continuous O_2 bubbling at 25°C for different MB concentrations in the membrane is shown by the data in Fig.13. (The lowest MB concentration required 45°C for adequate rate of lysis.) Additional results showing the increase of lysis rate with temperature are shown in Fig.14. These data are typical of prior work and do not show the major role of the hydrodynamic forces. However, the results in Fig.15 were obtained by irradiating for different periods of time, followed by dark bubbling with O_2 at 25°C.

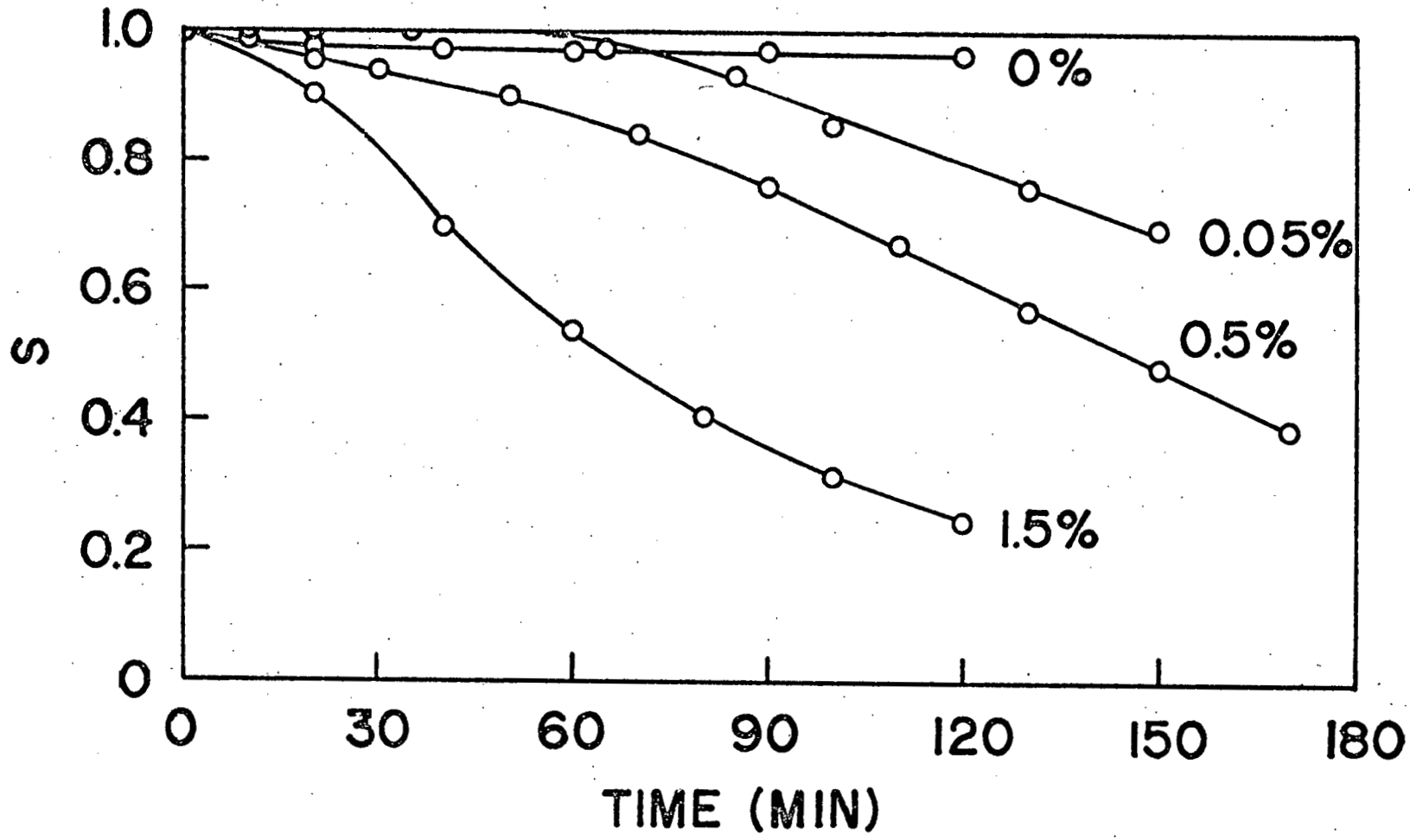

Figure 13. Lysis of egg lecithin liposomes by continuous red light irradiation with oxygen bubbling. The methylene blue concentration (w/w%) in the membrane is given next to each curve. All 25°C except 0.05% at 45°C.

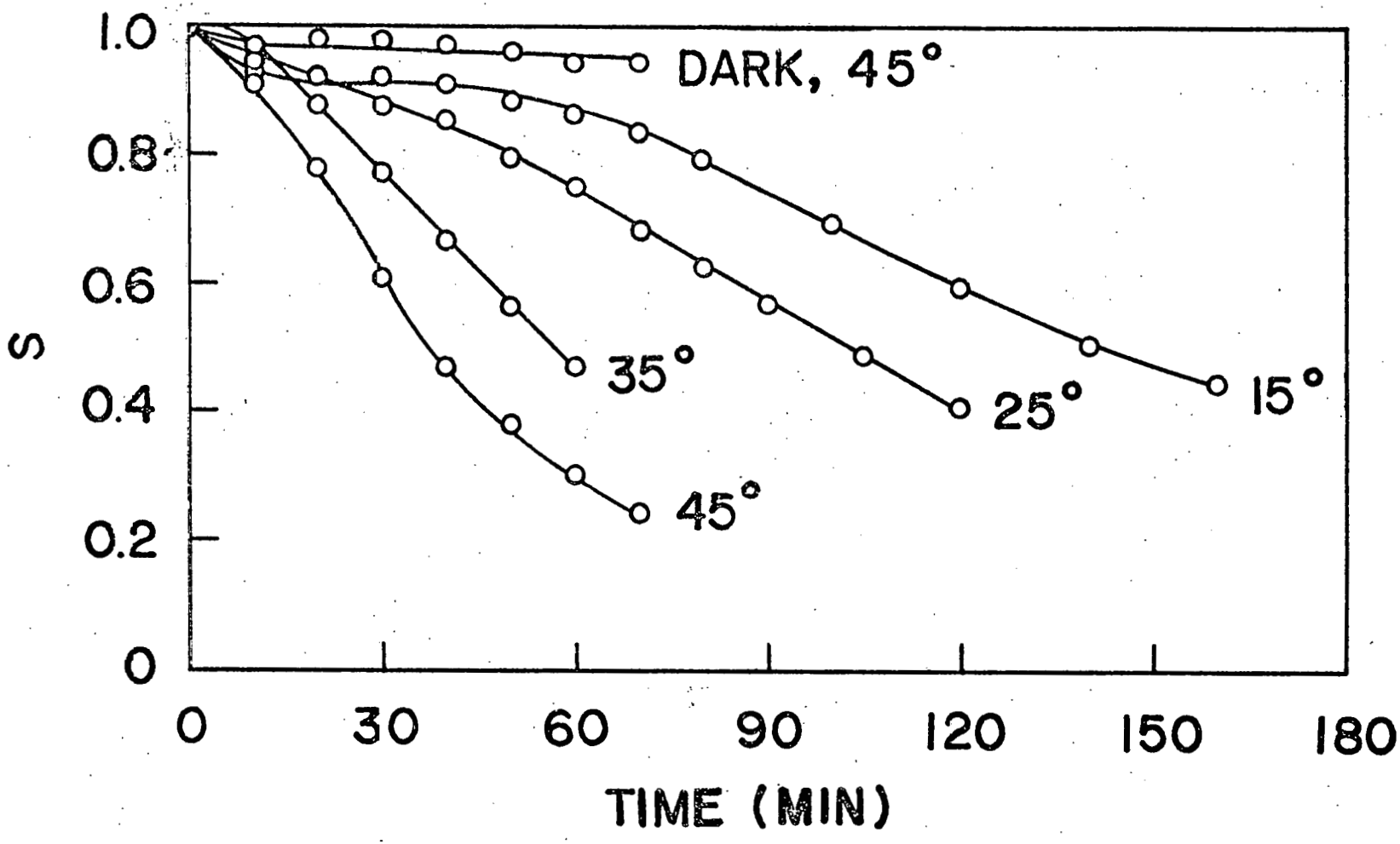

Figure 14. Temperature dependence of liposome lysis for continuous red light irradiation and oxygen bubbling. Egg lecithin liposomes with 0.5% methylene blue in the membrane.

In this case there was significant lysis in the dark, followed by saturation at a level determined by the fluence. A similar result is shown for liposomes irradiated in the presence of MB in the external aqueous phase instead of in the membrane. (The MB concentration was approximately the same as the suspension of 1.5% MB liposomes.) The results demonstrate that a significant part of the damage involves hydrodynamic forces that are photosensitized by MB. The results in Fig.16 provide additional information about the photochemical stage. The protection by 0.1M azide ion and 0.1M DABCO and the enhanced lysis rate in D_2O are indicative of O_2^* involvement. Bubbling with N_2 led to a lesser degree of protection, suggesting the presence of O_2 in the membrane not removed by prior N_2 bubbling. However, the lysis rate induced by bubbling was almost the same for O_2 and N_2 . The data in Fig.17 show that the dark lysis rate after a short irradiation with O_2 saturation was approximately the same for subsequent bubbling with N_2 and O_2 . Furthermore, the dark lysis rate was faster for the higher bubbling rate and changed from the lower rate to the higher when the bubbling rate was increased during the dark stage. These findings provide clear evidence that MB photosensitizes the liposome membrane to subsequent hydrostatic damage and that O_2^* is a major factor in the photolytic stage of the process.

A kinetics model for the photolysis process has been developed by assuming that photosensitization leads to damaged but intact liposomes that are subsequently lysed by hydrostatic interaction. The analysis can be simplified by assuming that negligible lysis takes place during the short irradiation period, in which case the number of damaged liposomes at the end of the irradiation period (t_a) is given by:

$$N_a' = N_o(1 - e^{-\alpha I_o t_a}) \qquad (15)$$

where I_o is the incident fluence rate, N_o is the initial number of liposomes, and α is proportional to the temperature, the O_2 concentration, and the MB concentration in the liposome membrane. The differential equation for the conversion of damaged liposomes is:

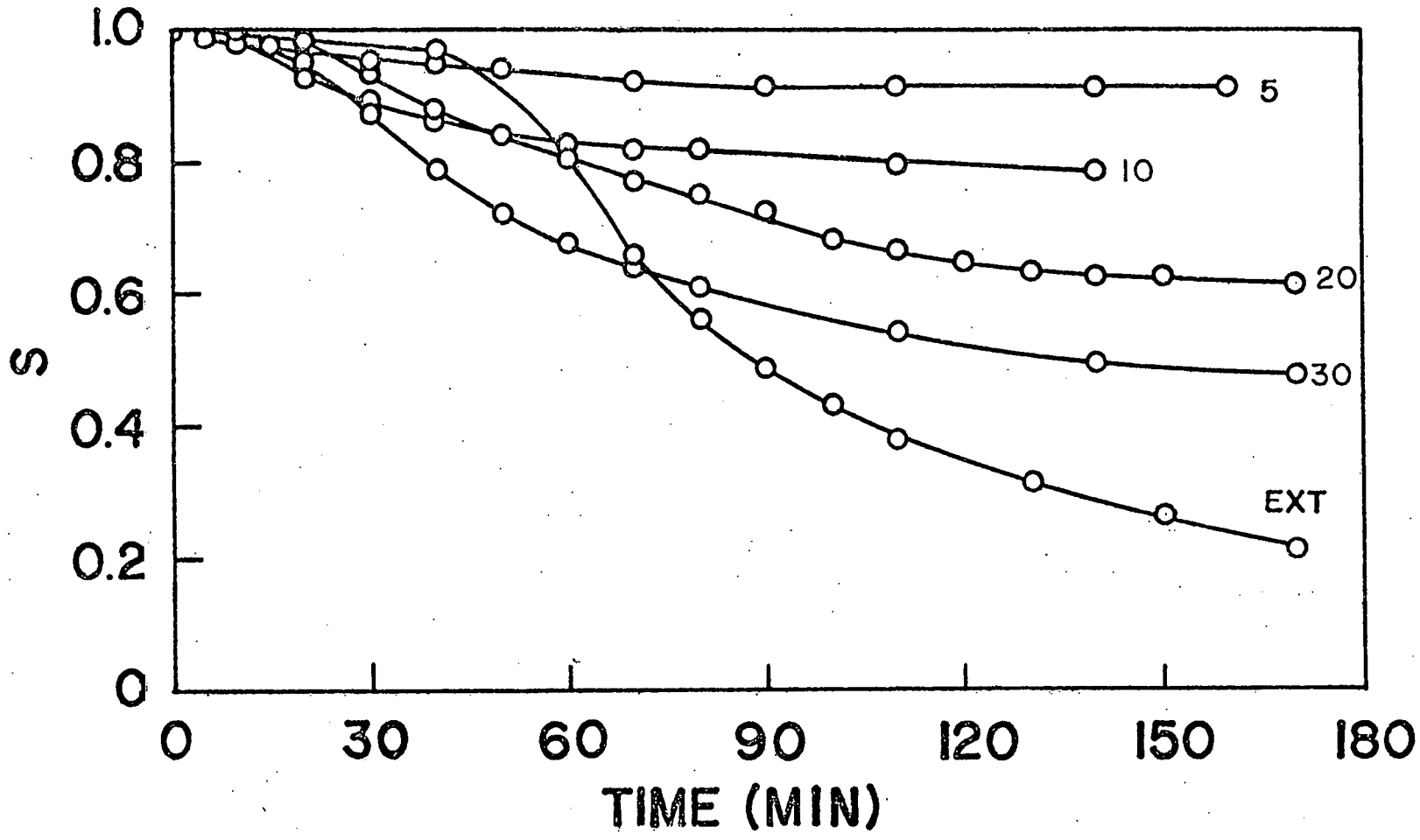

Figure 15. Liposome lysis by oxygen bubbling after red light irradiation for the time indicated next to each curve (minutes). Egg lecithin liposomes with 0.5% methylene blue in the membrane at 25°C. The methylene blue was in the external medium in the run EXT which was in the dark after 70 min.

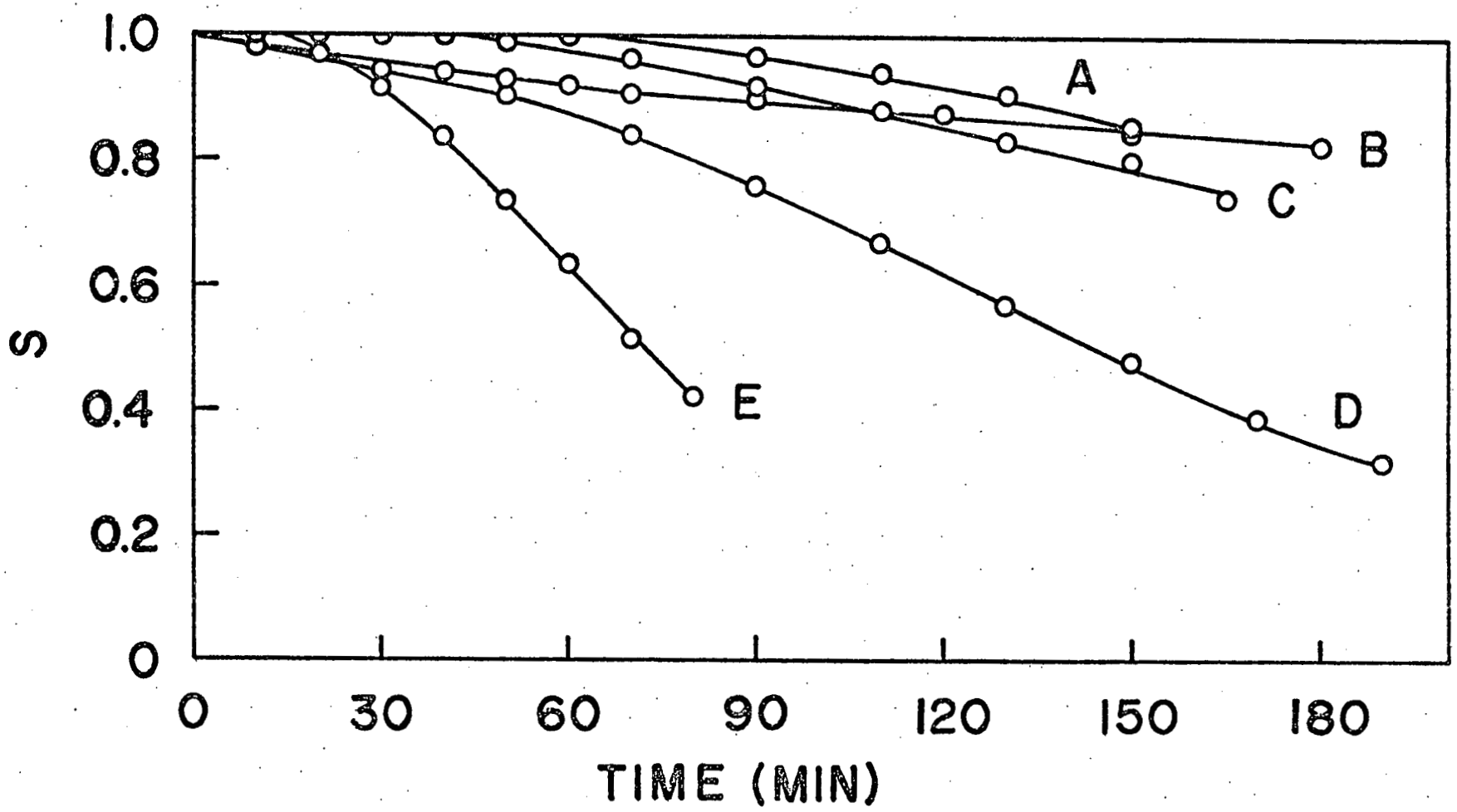

Figure 16. Lysis of egg lecithin liposomes with 0.5% methylene blue in the membrane with continuous red light irradiation and oxygen bubbling. A. with 0.1 M DABCO ; B. with 0.1 M azide ; C. N_2 saturation ; D. O_2 saturation ; E. in D_2O ; all 25°C.

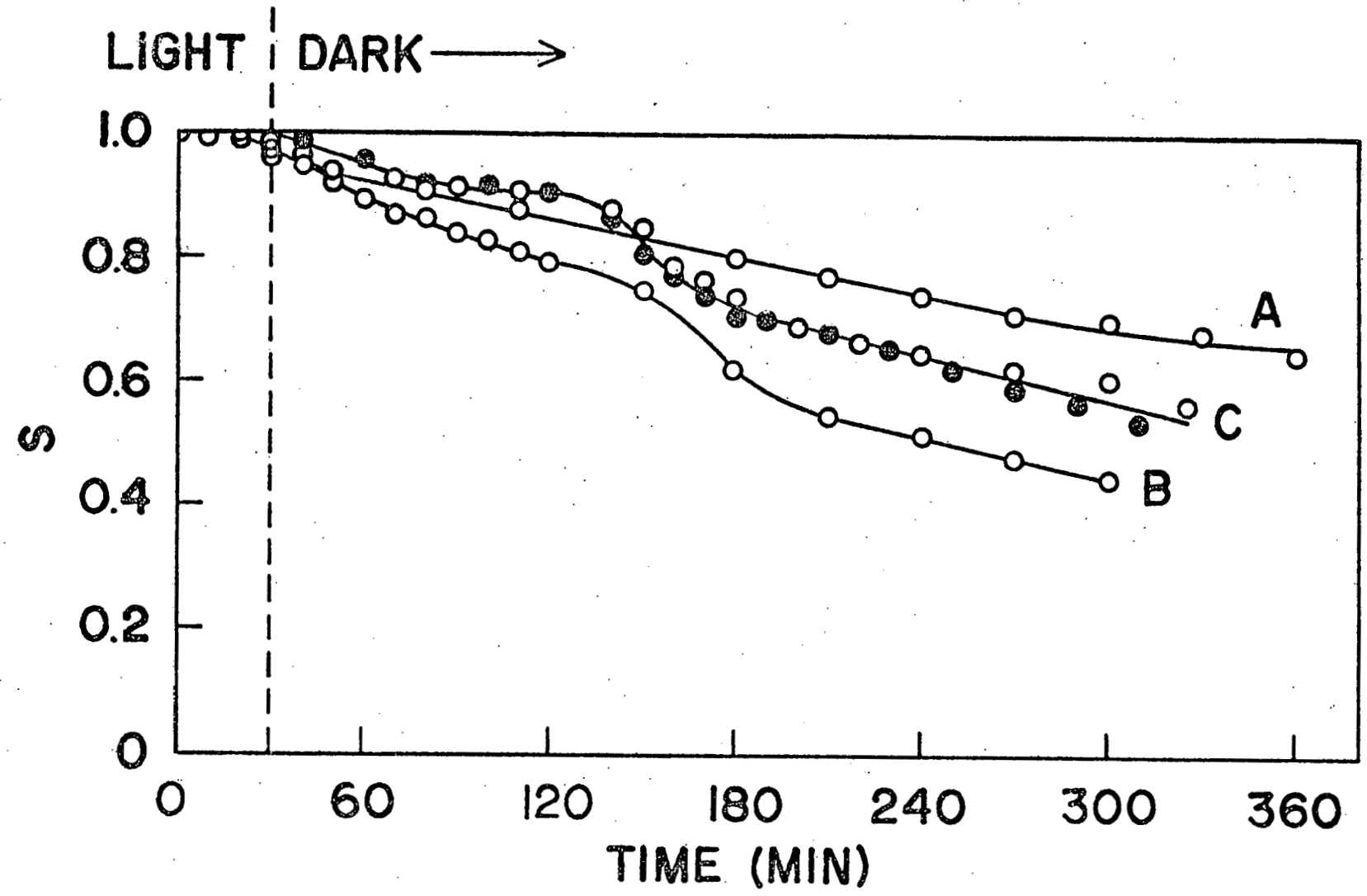

Figure 17. Effect of bubbling rate and gas on lysis of egg lecithin liposomes with 0.5% methylene blue in the membrane. The vertical dashed line indicates the end of the irradiation period with O_2 bubbling.
A. O_2 bubbling at 12 ml/min; B. O_2 bubbling at 25 ml/min.
C. Changed from 12 ml/min to 25 ml/min bubbling rate at 140 min:
O O_2 bubbled ; ● N_2 bubbled. All 25°C.

$$dN''/dt = \beta N' \qquad (16)$$

where N" is the number of lysed liposomes and β is proportional to the bubbling rate (or other hydrodynamic damage). However, for the present assumptions the loss of the damaged liposomes by lysis at $t>t_a$ is given by:

$$N'(t>t_a) = N'_a e^{-\beta(t-t_a)} \qquad (17)$$

leading to:

$$N''(t>t_a) = N'_a[1 - e^{-\beta(t-t_a)}] \qquad (18)$$

The surviving number of intact liposomes is N_o-N" , corresponding to the surviving fraction:

$$S = 1 - (1 - e^{-\alpha I_o t_a})[1 - e^{-\beta(t-t_a)}] \qquad (19)$$

According to Eq.(19), a plot of $\mathrm{Log}_e[(S-S_{sat})/(1-S_{sat})]$ vs $(t-t_a)$ should be linear, and all data for the same temperature and bubbling rate should fall on the same line. Here, S_{sat} is the survival after extended bubbling and t_a is the irradiation time prior to dark bubbling. The application to the data of Fig.15 is shown in Fig.18, where t_a ranged from 5 to 30 min. The good straight line is consistent with the key assumption of the model, that the extent of dark lysis is limited by the irradiation fluence. Another conclusion from Eq.(19) is the relationship:

$$S_{sat} = e^{-\alpha I_o t_a} \qquad (20)$$

The validity of Eq.(18) is shown by the upper right cut in Fig.18.

The case of continuous irradiation and bubbling (e.g. Fig.14) is more complicated analytically. As above, defining N, N', and N" as the numbers of original liposomes, photochemically damaged but intact liposomes, and lysed liposomes, respectively, the loss of original liposomes is given by:

$$dN/dt = -\alpha I_N N \qquad (21)$$

where I_N is the rate of light absorption by the original liposomes. If $I_N = (N/N_o)I_o$ (i.e. the N and N' types have equal absorptions), the solution to Eq.(21) is:

$$N(t) = N_o/[1 + \alpha I_o t] \qquad (22)$$

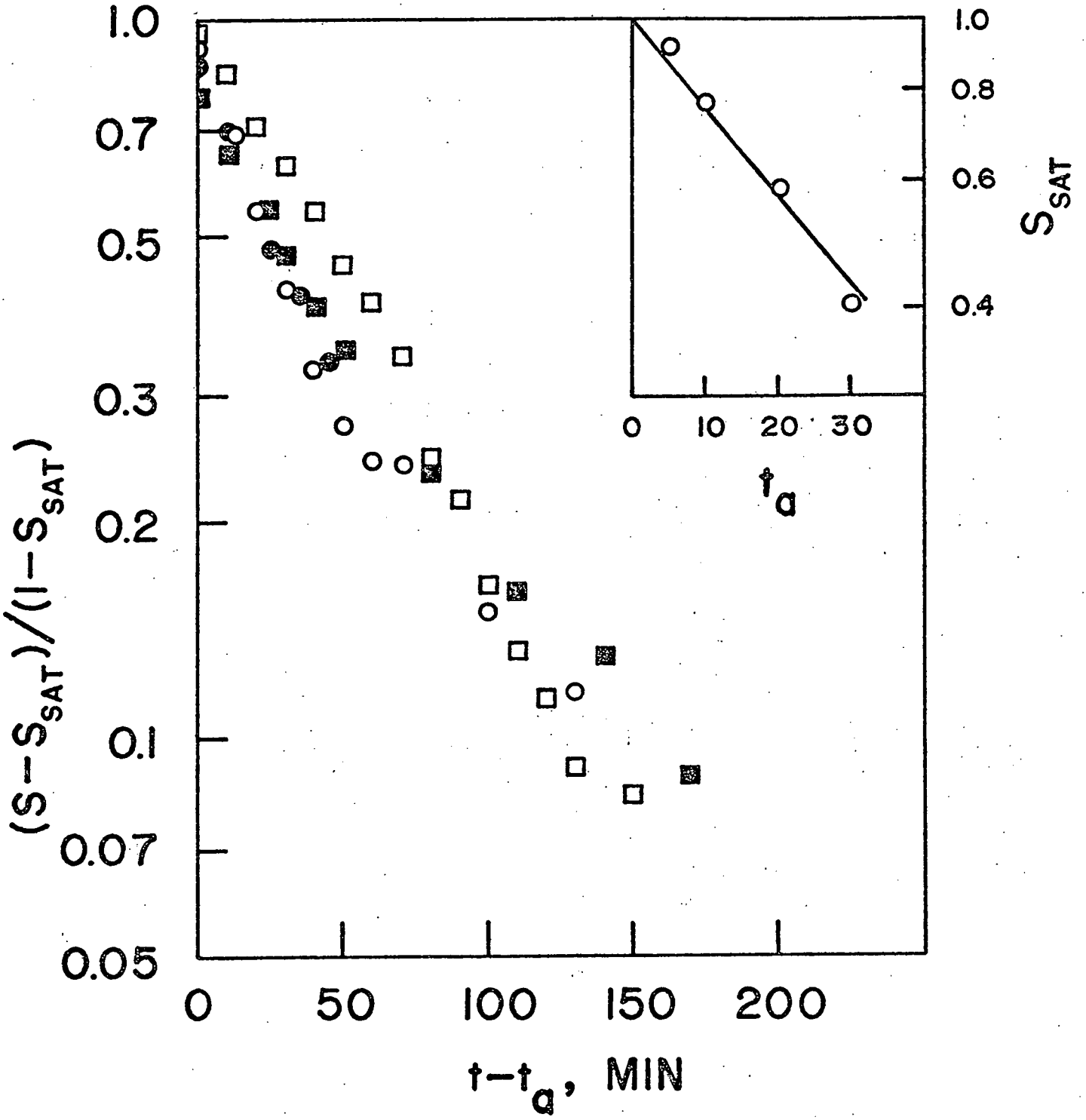

Figure 18. Plot of Figure 15 data according to Equation (19). t_a values: ◉ 5 min, ○ 10 min, □ 20 min, ▣ 30 min. Upper Right Plot of Equation (20).

The rate of formation and loss of the type N' liposomes is given by:

$$dN'/dt = \alpha(I_o/N_o)N^2 - \beta N' \qquad (23)$$

with the solution:

$$N'(t) = \alpha I_o N_o e^{-\beta t} \int_0^t \frac{e^{\beta t'}\, dt'}{(1+\alpha I_o t')^2} \qquad (24)$$

Substituting Eq.(24) in Eq.(16) and simplifying gives:

$$S(t) = e^{-\beta t}[1 + \beta \int_0^t \frac{e^{\beta t'}\, dt'}{(1+\alpha I_o t')} \,] \qquad (25)$$

An alternative form of Eq.(25) convenient for computation is:

$$S(X) = e^{-Ax}[e^A + AEi(-A) - AEi(-Ax)] \qquad (26)$$

where $x \equiv (1+\alpha I_o t)$, $A \equiv \beta/\alpha I_o$ and $-Ei(-y) \equiv \int_y^\infty (e^{-t}/t)dt$

Theoretical plots of S vs $(\alpha I_o t)$ for different values of A as calculated with an HP-85 microcomputer are shown in Fig.19. The value of A is determined by the relative rate of lysis by hydrostatic action compared to the damaging effect of the light. The theoretical plot for A = 0.3 has the same general dependence on time as Fig.13 (1.5% MB) and Fig.15 (30 min irradiation), when the photochemical fluence was high. A more detailed fitting of Eq.(26) to data is being continued in current work.

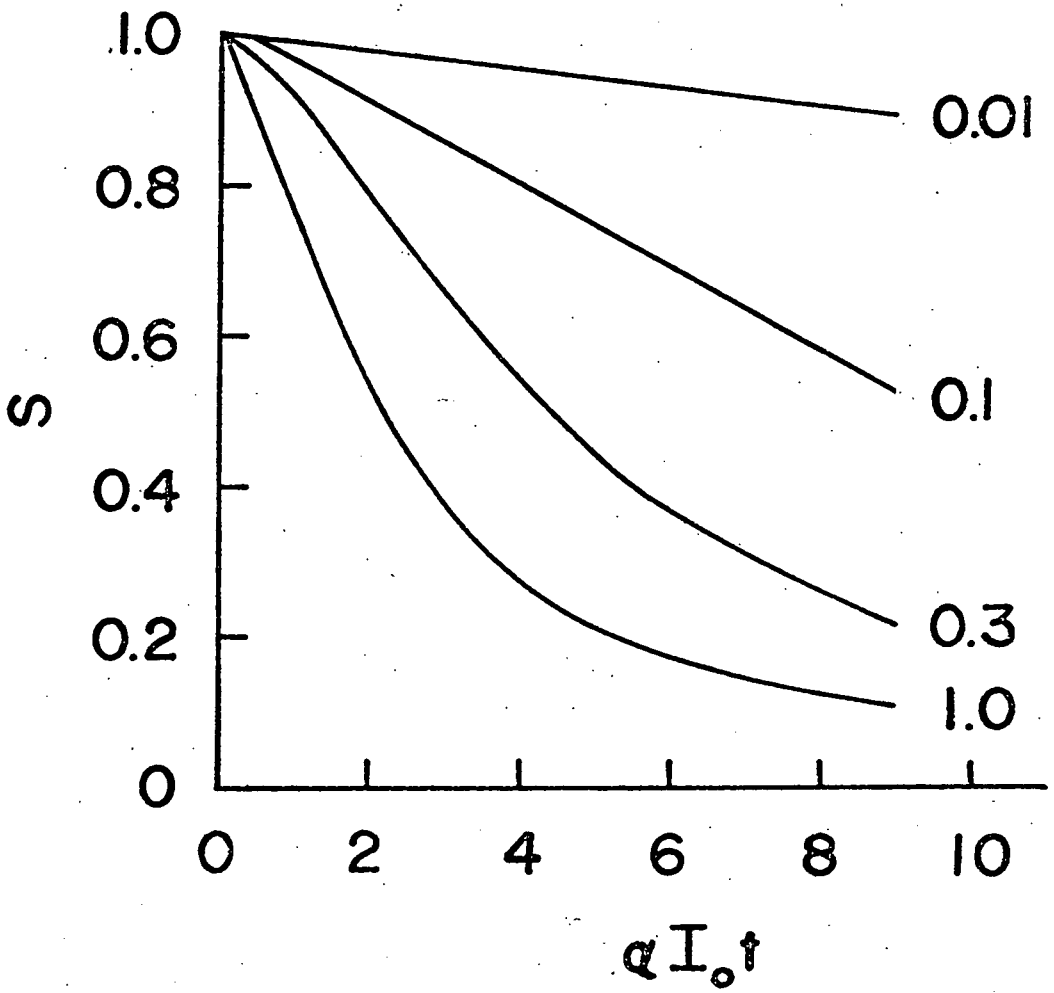

Figure 19. Theoretical liposome lysis curves for continuous irradiation and bubbling according to Equation (26). The number next to each curve is the parameter $\beta/\alpha I_o$.

References

1. B.Finnstrom,F.Tfibel and L.Linqvist, Chem.Phys.Lett. 71, 312(1980).
2. D.V.Bent and E.Hayon, J.Am.Chem.Soc. 97, 2612(1975).
3. R.Klein, I.Tatischeff,M.Bazin and R.Santus, to be published.
4. J.C.Mialocq,E.Amouyal,A.Bernas and D.Grant, to be published.
5. T.B.Truong, J.Phys.Chem. 84, 960(1980).
6. M.Charlier and C.Helene, Photochem.Photobiol. 21, 31(1975).
7. L.I.Grossweiner,A.M.Brendzel and A.Blum, Chemical Physics 00, 000(198
8. F.D.Bryant,R.Santus and L.I.Grossweiner, J.Phys.Chem. 79, 2711(1975).
9. J.F.Baugher and L.I.Grossweiner, J.Phys.Chem. 81, 1349 (1977).
10. J.Y.Lee,J.F.Baugher and L.I.Grossweiner, Photochem.Photobiol. 29, 867(1979).
11. A.D.McLaren and R.A.Luse, Science 134, 836 (1961).
12. K.Dose, Photochem.Photobiol. 6, 437(1967).
13. L.I.Grossweiner,A.G.Kaluskar and J.F.Baugher, Int.J.Radiat.Biol. 29,1(1976).
14. L.I.Grossweiner, Curr.Topics Radiat.Res.Quart. 11, 141(1976).
15. T.K.Rathinasamy and L.G.Augenstein, Biophys.J. 8, 1275(1968).
16. L.I.Grossweiner, Photochem.Photobiol. 00, 000(1981).
17. F.Dall'Acqua,S.Caffieri and G.Rodighiero, Photochem.Photobiol. 27, 77(1978).
18. F.Dall'Acqua,S,Marciani,L.Ciavatta and G.Rodighiero, Z.Naturforsch. 26b, 561 (1971).
19. I.M.Klotz,F.M.Walker and R.B.Pivan, J.Am.Chem.Soc. 68, 1486(1946).
20. D.Becker,J.L.Redpath and L.I.Grossweiner, Radiat.Res.73, 51(1978).
21. L.I.Grossweiner, Photochem.Photobiol. 26, 309(1977).
22. F.Hutchinson and J.Arena, Radiat.Res. 13, 137(1960).
23. W.Poppe and L.I.Grossweiner, Photochem.Photobiol. 22, 217(1975).
24. R.V.Bensasson,E.J.Land and C.Salets, Photochem.Photobiol. 27, 273(1978).
25. P.C.Beaumont et al.,Biochim.Biophys.Acta 608, 259(1980).
26. S.Cannistraro and A.Van de Vorst, Biochim.Biophys.Acta 476, 166(1977).
27. N.J.de Mol and G.M.J.Beijersbergen van Henogouwen, Photochem. Photobiol. 30, 331(1979).
28. T.Ito, Photochem.Photobiol. 28, 493(1978).
29. R.S.Stern et al., N.Eng.J.Med. 300, 809(1979).
30. L.Dubertret et al., Brt.J.Dermatol. 101, 379(1978).

31. R.D.Ley,D.D.Grube and R.J.M.Fry, Photochem.Photobiol. 25, 265(1977).

32. D.Averbeck,E.Moustacchi and E. Bisagni, Biochim.Biophys.Acta 518, 464 (1978).

33. R.Muller-Runkel and L.I.Grossweiner, Photochem.Photobiol. 33, 399(1981).

34. A.S.Fleischer,L.C.Harber,J.S.Cook and R.L.Baer, J.Invest.Dermatol. 46, 505(1966).

35. F.Dall'Acqua, S.Marciani Magno, F. Zambion and G.Rodighiero, Photochem.Photobiol. 29, 489(1979).

36. F.Dall'Acqua, M.Terbojevich, S.Marciani, D.Vedaldi and M.Recher, Chem.Biol.Interact. 21, 103(1978).

37. G.Rodighiero et al.,Biochim.Biophys.Acta 217, 40(1970).

38. L.I.Grossweiner and K.C.Smith, Photochem.Photobiol. 33, 317(1981).

39. L.I.Grossweiner, In "Oxygen and Oxyradicals in Chemistry and Biology" (Ed. M.A.J.Rodgers and E.L.Powers),Academic Press, New York, 1981, pp.000-000.

40. S.M.Anderson and N.I.Krinsky, Photochem.Photobiol. 18, 403(1973).

41. D.I.Roshchupkin et al., Photochem.Photobiol. 21, 63(1975).

42. K.Suwa, T.Kimura and A.P.Schaap, Photochem.Photobiol. 28, 469(1978).

43. R.Muller-Runkel,J.Blais and L.I.Grossweiner, Photochem.Photobiol. 33, 683(1981).

Summary of Project Activity

Project Activity

The expenditure of scientific effort and funds was consistent with the technical program in the Renewal Proposal and the current budget.

Scientific Salaries

Dr. Leonard I. Grossweiner (Professor)
2 months Summer 1981

Dr. Avrom M. Brendzel (Research Associate)
100% time October 1, 1980 - May 31, 1982

Non-Salaried Research Staff

Dr. Renate Muller-Runkel (Graduate Assistant)
1980-81 academic year

Foreign Travel

None